

## THE GAS CHROMATOGRAPH MASS SPECTROMETER FOR THE HUYGENS PROBE

H. B. NIEMANN<sup>1,\*</sup>, S. K. ATREYA<sup>2,\*</sup>, S. J. BAUER<sup>3,\*</sup>, K. BIEMANN<sup>4,\*</sup>, B. BLOCK<sup>2</sup>, G. R. CARIGNAN<sup>2,\*</sup>, T. M. DONAHUE<sup>2,\*</sup>, R. L. FROST<sup>9</sup>, D. GAUTIER<sup>5,\*</sup>, J. A. HABERMAN<sup>1</sup>, D. HARPOLD<sup>1</sup>, D. M. HUNTEN<sup>6,\*</sup>, G. ISRAEL<sup>7,\*</sup>, J. I. LUNINE<sup>6,\*</sup>, K. MAUERSBERGER<sup>8,\*</sup>, T. C. OWEN<sup>10,\*</sup>, F. RAULIN<sup>11,\*</sup>, J. E. RICHARDS<sup>1</sup>, S. H. WAY<sup>1</sup>

<sup>1</sup>National Aeronautics and Space Administration, Greenbelt, MD 20771, USA (E-mail: Hasso.B.Niemann@nasa.gov; Fax: +1 301 614-6406); <sup>2</sup>University of Michigan, Ann Arbor, MI 48109, USA; <sup>3</sup>Institute for Meteorology and Geophysics, University of Graz, A-8010 Graz, Austria; <sup>4</sup>Massachusetts Institute of Technology, Cambridge, MA 01239, USA; <sup>5</sup>Observatoire de Paris-Meudon, F-92195 Meudon Cedex, France; <sup>6</sup>University of Arizona, Tucson, AZ 85716, USA; <sup>7</sup>Service d'Aéronomie du CNRS, F-91371 Verrières le Buisson Cedex, France; <sup>8</sup>Max Planck Institute, Kernphysik, D-69029 Heidelberg, Germany; <sup>9</sup>University of Alabama, CMC, 817 22nd Street, South Birmingham, AL 35205, USA; <sup>10</sup>University of Hawaii, Honolulu, HI 96822, USA; <sup>11</sup>Laboratoire Interuniversitaire des Systèmes Atmosphériques, Université Paris 12 et Paris 7, Avenue du général de Gaulle, F-94010 Creteil Cedex, France

Received 11 September 1998; Accepted in final form 25 May 1999

**Abstract.** The Gas Chromatograph Mass Spectrometer (GCMS) on the Huygens Probe will measure the chemical composition of Titan's atmosphere from 170 km altitude (~1 hPa) to the surface (~1500 hPa) and determine the isotope ratios of the major gaseous constituents. The GCMS will also analyze gas samples from the Aerosol Collector Pyrolyser (ACP) and may be able to investigate the composition (including isotope ratios) of several candidate surface materials.

The GCMS is a quadrupole mass filter with a secondary electron multiplier detection system and a gas sampling system providing continuous direct atmospheric composition measurements and batch sampling through three gas chromatographic (GC) columns. The mass spectrometer employs five ion sources sequentially feeding the mass analyzer. Three ion sources serve as detectors for the GC columns and two are dedicated to direct atmosphere sampling and ACP gas sampling respectively. The instrument is also equipped with a chemical scrubber cell for noble gas analysis and a sample enrichment cell for selective measurement of high boiling point carbon containing constituents. The mass range is 2 to 141 Dalton and the nominal detection threshold is at a mixing ratio of  $10^{-8}$ . The data rate available from the Probe system is 885 bit/s. The weight of the instrument is 17.3 kg and the energy required for warm up and 150 minutes of operation is 110 Watt-hours.

\*Member Investigation Team.



*Space Science Reviews* **104**: 553–591, 2002.

© 2003 Kluwer Academic Publishers. Printed in the Netherlands.

**Table of Contents**

|      |  |     |
|------|--|-----|
| 1    | Scientific Objectives  | 555 |
| 1.1  | Introduction   | 555 |
| 1.2  | Atmospheric composition: argon, isotopes and organic compounds | 555 |
| 1.3  | Descent sequence   | 560 |
| 1.4  | Surface science  | 560 |
| 2    | Instrument Description   | 561 |
| 2.1  | General  | 561 |
| 2.2  | Gas sampling system  | 565 |
| 2.3  | Aerosol collector pyrolyser analysis                           | 569 |
| 2.4  | Post surface impact analysis                                   | 570 |
| 2.5  | Ion sources  | 570 |
| 2.6  | Quadrupole mass filter and ion detector                        | 572 |
| 2.7  | Pumping systems  | 574 |
| 2.8  | Electronic system  | 574 |
| 2.9  | Mechanical configuration                                       | 577 |
| 2.10 | Sampling strategy  | 580 |
| 2.11 | Data format  | 581 |
| 3    | Instrument Calibration   | 582 |
| 3.1  | Gas mixtures used in GCMS sensor characterization              | 584 |
| 3.2  | Post-launch calibration  | 584 |
| 4    | Post Launch Performance and Testing                            | 584 |
| 5    | Expected Results and Measurement Accuracy                      | 586 |
|      | Acknowledgements   | 588 |
|      | References   | 589 |

## 1. Scientific Objectives

### 1.1. INTRODUCTION

Titan is unique in the solar system in several respects. The dense atmosphere is still chemically reducing, even though Titan is small enough to allow hydrogen to escape readily from its gravitational field. The major constituents of the atmosphere, nitrogen and methane, are continuously broken apart by a combination of solar UV, impinging electrons from Saturn's magnetosphere, and a steady flux of cosmic rays. The resulting molecular fragments recombine to form a variety of new species, many of which were detected for the first time by Voyager 1 (Broadfoot *et al.*, 1981; Hanel *et al.*, 1981; Kunde *et al.*, 1981; Samuelson *et al.*, 1981, 1983; Lutz *et al.*, 1983; Bézard *et al.*, 1993). The existence of still more complex compounds is manifested by the ubiquitous, surface-hiding aerosol blanket. In addition to hydrocarbons and nitriles, the atmosphere is known to contain CO, CO<sub>2</sub> and externally delivered H<sub>2</sub>O (see reviews by Hunten *et al.*, 1984; Morrison *et al.*, 1986; Lunine *et al.*, 1989). The origin of this atmosphere, the processes involved in its evolution, the end products and their subsequent fate as they interact with the surface remain to be elucidated. A particularly interesting aspect of this investigation is the possible relevance of the chemical evolution currently occurring on Titan to some of the prebiotic syntheses that took place on the early Earth (Raulin *et al.*, 1992a; Owen *et al.*, 1997). It is the purpose of the GCMS to provide an accurate analysis (see Table 1) of Titan's atmospheric composition along the descent trajectory of the Huygens Probe. The instrument is a follow-on to others used in making measurements of the atmosphere of Venus (Niemann *et al.*, 1980) and Jupiter (Niemann *et al.*, 1992).

### 1.2. ATMOSPHERIC COMPOSITION: ARGON, ISOTOPES AND ORGANIC COMPOUNDS

Despite the great success of Voyager 1, the composition of Titan's atmosphere is still poorly known (Table 2). The present uncertainty in the methane mixing ratio and its variation with altitude can be resolved from the continuous recording of mass spectra by the GCMS during the Probe's descent. The Voyager observations left open the possibility that several percent of some heavy, spectroscopically undetectable gas might be present (Samuelson *et al.*, 1981). Non-radiogenic argon (<sup>36</sup>Ar + <sup>38</sup>Ar) is the most likely candidate (Owen 1982); the mass spectrometer can detect it down to mixing ratios of 10–100 ppb. The mole fraction of argon that could remain undetectable in presently available observations has been steadily decreasing with improved treatment of the data, first to ≤10% (Strobel *et al.*, 1993), then to ≤6% (Courtin *et al.*, 1995), the same upper limit originally reported for the heterosphere by Broadfoot *et al.*, (1981), and most recently to 2.6% with an uncertainty of ±4.5% (Samuelson *et al.*, 1997). In fact, several percent of argon

TABLE 1  
Science objectives

|                                    |  |
|------------------------------------|--|
| Atmospheric composition            | Abundances of all constituents within the mass range of the instrument with mixing ratios $> 10^{-8}$ , selected species to $10^{-10}$ . |
| Atmospheric origin                 | Discrimination between primordial and radiogenic argon. Surface composition. Other noble gas abundances. Value of D/H.                   |
| Atmospheric and interior evolution | Major element isotopes. Surface composition. Noble gas abundances. CO vertical distribution.   |
| Chemical evolution                 | Abundances of organic compounds. Variations with altitude. Surface composition.  |

would be difficult to explain based on current models for the origin of Titan's atmosphere (Owen and Bar-Nun, 1995).

The full range of abundance and isotope data provided by the GCMS will be employed to study atmospheric origin and evolution. For example, the ratio  $^{14}\text{N}/^{15}\text{N}$  has been found to be 4.5 times the terrestrial value in Titan's HCN (Marten *et al.*, 1997; Owen *et al.*, 1998). Yet the value of  $^{12}\text{C}/^{13}\text{C}$  in HCN is normal (Hidayat *et al.*, 1997). This situation is reminiscent of Mars, where  $^{14}\text{N}/^{15}\text{N}$  is 1.6 times normal and  $^{12}\text{C}/^{13}\text{C}$  is again normal. It suggests that as much as 45 times the current amount of nitrogen on Titan has escaped from the satellite, while there must be a correspondingly large reservoir of carbon somewhere on Titan, presumably in the form of hydrocarbons. Such a reservoir is required in any case to replenish the  $\text{CH}_4$  that is continually being dissociated (Strobel, 1982; Yung *et al.*, 1984). The GCMS is ideally suited to attack this problem, as it can measure the relevant isotope ratios in a variety of compounds in Titan's atmosphere, including  $\text{N}_2$ , which is inaccessible to other instruments. It will even measure  $^{36}\text{Ar}/^{38}\text{Ar}$  to see if this ratio has also been affected by the same escape process that fractionated the nitrogen.

Once the relative importance of atmospheric escape and chemical exchange have been determined for nitrogen, it will be possible to establish the original value of D/H in Titan's methane. For example, if  $\text{D}/\text{H} \sim 2 \times 10^{-5}$ , the value in Saturn's hydrogen (Griffin *et al.*, 1996), it might favor a sub-nebula origin for most of Titan's atmosphere. The current best estimate of Titan's D/H is based on  $\text{CH}_3\text{D}$  measured in the  $\nu_6$  band by Infrared Space Observatory/Short Wavelength Spectrometer (ISO/SWS, Coustenis *et al.*, 1998a). The result,  $\text{D}/\text{H} = 7.5 \times 10^{-5}$ , is in agreement with the earlier ground-based infrared observations which gave  $\text{D}/\text{H} = 7.75 \pm 2.25 \times 10^{-5}$  (Orton, 1982). The central value thus appears to be approximately a factor of 3 greater than the Saturn D/H or the protosolar D/H as derived from the Galileo Probe Mass Spectrometer at Jupiter (Mahaffy *et al.*, 1998). On the other hand, it is about a factor of 4 lower than that on comets Halley

(Balsiger *et al.*, 1995; Eberhardt *et al.*, 1995), Hyakutake (Bockelee-Morvan *et al.*, 1998) and Hale-Bopp (Meier *et al.*, 1998) which all have a  $D/H \sim 30 \times 10^{-5}$ . The available evidence therefore suggests that comets could not have been the main source of Titan's atmosphere, contrary to the hypothesis of Griffith and Zahnle (1995). Instead, degassing of the icy planetesimals that accreted within Saturn's subnebula to form Titan seems implicated. Investigations of noble gas abundances and isotopes can shed further light on the origin of the atmosphere. For example, most of the neon on Titan may have come from the rocky fraction of the satellite, while krypton and xenon could have been contributed primarily by the ice, as on Earth (Owen and Bar-Nun, 1995). The dissociation of  $NH_3$  by the solar ultraviolet radiation (Atreya *et al.*, 1978) or by impact induced shock chemistry (McKay *et al.*, 1988) could have produced all of the  $N_2$  in Titan's present day atmosphere early in its accretionary history. A satisfactory resolution of the complex question of the origin and evolution of Titan's atmosphere requires, however, accurate in situ measurements of  $D/H$  as well as the abundance and isotopic ratios of argon, particularly  $^{40}Ar/^{36}Ar$ , as the current data are poorly constrained and model dependent.

The oxidized compounds offer other opportunities and challenges. The production of  $CO_2$  requires hydroxyl (OH) that may come either from the outside atmosphere (e.g., by bombarding ice particles or micrometeorites) or from internal sources (e.g., the reaction of  $CH_4$  with CO). The external source seems likely to be more efficient, but we don't know the flux of incoming particles. The recent detection of water vapor in Titan's upper atmosphere by ISO/SWS (Coustenis *et al.*, 1998a) is encouraging. The spectra can be fitted with a uniform  $H_2O$  mixing ratio of 0.4 ppb. The OH produced from the photolysis of  $H_2O$  would react with CO to produce  $CO_2$ . If some fraction of the nitrogen we now see in Titan's atmosphere was originally incorporated as  $N_2$ , one would expect a comparable amount of primordial CO. In that case, a significant amount of  $CO_2$  would have been produced and a corresponding deposit of 'dry ice' could now be present on the surface, intimately mixed with accumulated organic aerosols (Samuelson *et al.*, 1983; Owen and Gautier, 1989). Note, however, that the observed amount of  $H_2O$  seems insufficient for producing the observed  $CO_2$  by the conventional mechanism (i.e.,  $CO + OH \rightarrow CO_2$ ). It may be necessary to invoke an additional path, such as a reaction between the externally delivered  $H_2O$  and Titan's own methane (actually between OH, the photoproduct of  $H_2O$ , and the dissociation products of  $CH_4$ ). On the other hand, the situation regarding CO itself is in a less than satisfactory state. The first detection of CO was in the near infrared, i.e., the data yielded the CO abundance in Titan's troposphere (Lutz *et al.*, 1983). Their CO mixing ratio of  $\sim 50$  ppm was later confirmed by Muhleman *et al.*, (1984) and again by Gurwell and Muhleman (1995) who observed the J(1-0) transition of CO at 115 GHz. The microwave data pertain to the stratosphere, so a uniform mixing ratio with altitude is indicated by the above authors. Courtin *et al.*, (1998) have performed a more sophisticated analysis of the near infrared absorptions but obtained the same result.

TABLE 2  
Atmospheric composition of Titan\*

| Constituent                         | Mixing Ratio                          | Reference   |
|-------------------------------------|---------------------------------------|---|
| Major Species (global values)       |                                       |   |
| N <sub>2</sub>                      | 0.85–0.98                             | Hanel <i>et al.</i> , 1981  |
| Ar                                  | 0.026 ± 0.045                         | Samuelson <i>et al.</i> , 1997  |
|                                     | ≤0.06                                 | Broadfoot <i>et al.</i> , 1981  |
| CH <sub>4</sub>                     | ≤0.15 at surface                      | Courtin <i>et al.</i> , 1995  |
| Minor Species                       |                                       |   |
| <i>H Group</i>                      |                                       |   |
| H <sub>2</sub>                      | 2–6 × 10 <sup>-3</sup>                | de Bergh <i>et al.</i> , 1988   |
| D/H                                 | 7.8 ± 2.3 × 10 <sup>-5</sup>          | Orton, 1992; Coustenus <i>et al.</i> , 1998b  |
| <i>CN Group</i>                     |                                       |   |
|                                     |                                       | Coustenus and Bézard, 1995; Bézard <i>et al.</i> , 1993   |
| C <sub>2</sub> N <sub>2</sub>       | ~ 2 × 10 <sup>-8</sup>                |   |
| C <sub>4</sub> N <sub>2</sub>       | condensed phase                       |   |
| <i>C-N-H Group</i>                  |                                       |   |
|                                     |                                       | Coustenus and Bézard, 1995; Bézard <i>et al.</i> , 1993   |
| HCN                                 | ~ 2 × 10 <sup>-7</sup> (global)       |   |
| HC <sub>3</sub> N                   | ~ 3 × 10 <sup>-8</sup>                |   |
| CH <sub>3</sub> CH                  | 1–5 × 10 <sup>-9</sup> (global)       |   |
| <i>Oxygen Group (global values)</i> |                                       |   |
| CO                                  | 0.4–6 × 10 <sup>-5</sup>              | Lutz <i>et al.</i> , 1983; Muhleman <i>et al.</i> , 1984; Gurwell and Muhleman, 1995; Marten <i>et al.</i> , 1988; Hidayat <i>et al.</i> , 1998 |
| CO <sub>2</sub>                     | ~ 1 × 10 <sup>-8</sup>                | Samuelson <i>et al.</i> , 1983  |
| H <sub>2</sub> O                    | 4 × 10 <sup>-10</sup> (global)        | Coustenus <i>et al.</i> , 1998a   |
| <i>C-H Group</i>                    |                                       |   |
|                                     |                                       | Coustenus and Bézard, 1995; Bézard <i>et al.</i> , 1993; Coustenus <i>et al.</i> , 1998b  |
| C <sub>2</sub> H <sub>6</sub>       | 1–2 × 10 <sup>-5</sup>                |   |
| C <sub>3</sub> H <sub>8</sub>       | ~ 10 <sup>-6</sup>                    |   |
| C <sub>2</sub> H <sub>2</sub>       | 2–6 × 10 <sup>-6</sup>                |   |
| C <sub>2</sub> H <sub>4</sub>       | 10 <sup>-6</sup>                      |   |
|                                     | 8.0 ± 2 × 10 <sup>-8</sup> (global)   |   |
| CH <sub>3</sub> C <sub>2</sub> H    | ~ 3 × 10 <sup>-8</sup>                |   |
|                                     | 8.0 ± 1.5 × 10 <sup>-9</sup> (global) |   |
| C <sub>4</sub> H <sub>2</sub>       | ~ 2 × 10 <sup>-8</sup>                |   |
|                                     | 1.5 ± 0.2 × 10 <sup>-9</sup> (global) |   |

\*Values at other latitudes and seasons likely to be different.

However, Marten *et al.*, (1988) and Hidayat *et al.*, (1998) using microwave observations of transitions from higher rotational levels derived a lower value for the CO abundance and found evidence for a decrease of CO with altitude. Noll *et al.*, (1996), studying the 5 micron spectrum, derived a value of only 10 ppm for CO. Considering the importance of CO in the models of the origin and evolution of Titan's atmosphere, the GCMS will investigate the chemistry of CO on Titan by measuring the abundance of this gas at the four altitudes at which atmospheric GC samples are taken.

The drivers for the chemistry on Titan are solar ultraviolet radiation, the charged particle induced chemistry when Titan is immersed in Saturn's magnetosphere, and galactic cosmic rays, especially for lower atmospheric chemistry. The chemistry of CH<sub>4</sub> on Titan proceeds, to some extent, in a manner similar to that proposed for Jupiter, with the exception that H<sub>2</sub> is replaced by N<sub>2</sub> as the major gas. The stable hydrocarbons resulting from the CH<sub>4</sub> photochemistry are C<sub>2</sub>H<sub>6</sub>, C<sub>2</sub>H<sub>2</sub>, and C<sub>2</sub>H<sub>4</sub>. Subsequent reactions involving C<sub>2</sub>H<sub>2</sub> result in the formation of methylacetylene or allene (C<sub>3</sub>H<sub>4</sub>), and polynes (C<sub>2n</sub>H<sub>2n</sub>, n = 2, 3, 4 . . .). Propane C<sub>3</sub>H<sub>8</sub>, butane C<sub>4</sub>H<sub>10</sub> and other heavier hydrocarbons are expected to be formed following the reaction of the radical CH<sub>3</sub> with C<sub>2</sub>H<sub>5</sub>, C<sub>3</sub>H<sub>7</sub>, etc.

Lower mixing ratios are expected with an increasing number of C atoms, but available observations paint a more complex picture. Careful reanalysis of the Voyager data by Coustenis and colleagues has revealed striking variations in abundances of minor constituents with latitude on Titan (Coustenis and Bézard, 1995 and references therein). At 50°N, they find the following in order of increasing abundance: C<sub>4</sub>H<sub>2</sub>, C<sub>2</sub>N<sub>2</sub>, HC<sub>3</sub>N, C<sub>3</sub>H<sub>4</sub>, C<sub>3</sub>H<sub>8</sub>, C<sub>2</sub>H<sub>8</sub>, HCN, C<sub>2</sub>H<sub>2</sub>, C<sub>2</sub>H<sub>6</sub>. Abundances measured at this latitude can be over 17 times the values at southern latitudes. The abundances measured by the GCMS along the Probe trajectory can be used to calibrate the remote measurements by the Composite Infrared Spectrometer (CIRS) on the Cassini Orbiter, allowing analysis of these variations over the globe during a season different from the one sampled by Voyager 1.

Unlike Jupiter, the CH<sub>4</sub> chemistry on Titan is not isolated, as the above list of constituents shows (cf. Table 2). Atomic nitrogen produced on dissociation of N<sub>2</sub> reacts with CH<sub>4</sub> and products of its photochemistry, CH<sub>3</sub> and CH<sub>2</sub>, to produce HCN. Photolysis of HCN produces CN. The reactions of CN with CH<sub>4</sub>, CN (or HCN) C<sub>2</sub>H<sub>2</sub> and C<sub>2</sub>H<sub>4</sub> yield, respectively, HCN, C<sub>2</sub>N<sub>2</sub>, HC<sub>3</sub>N, and C<sub>2</sub>H<sub>3</sub>CN (not yet detected). Reactions of CN with the other hydrocarbons result in the formation of additional nitriles such as CH<sub>3</sub>CN. Other possible nitriles with mixing ratios in the range 10<sup>-8</sup> to 10<sup>-9</sup> are: C<sub>2</sub>H<sub>5</sub> - N, CH<sub>2</sub> = CH - CN, CH<sub>3</sub>C ≡ C - CN and HC<sub>4</sub> - CN. Lower mole fractions are expected for nitriles at higher molecular weight. For comprehensive discussions of the models of chemical pathways in Titan's atmosphere, the reader is referred to Yung *et al.*, 1984; Atreya, 1986; Lunine *et al.*, 1989; Toublanc *et al.*, 1995; Lara *et al.*, 1996.

The GCMS will approach this analysis problem in four ways: by taking mass spectra continuously, thereby measuring every m/e peak from 2 to 141 Dalton; and

by making discrete GC analyses at various altitudes, including sample enrichment, thereby permitting both greater sensitivity and specificity in identification at those points. A third approach is possible in collaboration with the ACP experiment (see Israel *et al.*, this volume), and a fourth possibility exists (as described below) if the Probe survives the landing.

### 1.3. DESCENT SEQUENCE

The mass spectrometer will make direct measurements continuously from initiation of experiments until landing at a sampling rate of 5 ms. A minimum of five GC samples will be taken, one immediately after the opening of the inlet valve, another one in the lower stratosphere, a third near 60 km (where concentrations of most complex trace gases are thought to be the highest) and two more below 60 km altitude. One of the latter will be devoted to analysis of the output from the aerosol pyrolysis experiment and the other taken near the atmospheric temperature minimum to provide the best CO/N<sub>2</sub> separation. A sixth sample can be taken close to the surface if the nominal descent time is maintained. Its purpose is to characterize conditions near the ground, especially to search for evidence of the vapor phases of possible surface condensates. The timing will be adjusted to ensure read out of the GCMS prior to impact for the nominal descent scenario.

### 1.4. SURFACE SCIENCE

Titan has the largest unexplored surface in the solar system. This surface is currently being studied at a very low spatial resolution (~300 km) by ground-based and Hubble Space Telescope observations through near-IR windows (Smith *et al.*, 1996 and references therein, Combes *et al.*, 1997; Gibbard *et al.*, 2001) and by means of radar (Muhleman *et al.*, 1995). Owing to the presence of Titan's thick, chemically active atmosphere, the surface of this satellite must be one of the most unusual we are ever likely to see. This surface must contain or conceal a reservoir for atmospheric methane, since the present atmospheric abundance of this gas will be destroyed by photochemistry in just 10<sup>7</sup> years. Unless we just happen to be living at the time when Titan's original methane comes to an end, the surface (or sub-surface) must provide a means for replenishing this gas. The products of atmospheric chemistry will accumulate on Titan's surface over geologic time, with the potential of producing deposits with depths on the order of a kilometer or more. If liquids are present, one can imagine their influence on the landscape through erosion, and the possibility that further chemical processing also occurs in them (Raulin *et al.*, 1995).

Three extreme models for Titan's surface have been proposed:

- a global ocean of hydrocarbons dominated by ethane but containing methane, nitrogen, carbon monoxide and many other dissolved species;
- a global covering of precipitated aerosols;
- an icy landscape dominated by impact craters, perhaps including rocky debris.



It is now clear that the first of these models cannot be correct. A solid surface with lakes or seas of liquid hydrocarbons and some areas dominated by aerosol deposits is more consistent with existing data (Lunine, 1993, 1994; Lorenz, 1993; Smith *et al.*, 1996).

If Huygens lands in a liquid, a compositional analysis with the GCMS is straightforward. Mass spectra of evaporating liquid showing the relative abundances of nitrogen, ethane, methane, argon and other noble gases, simple hydrocarbons, nitriles and oxides would be an outstanding contribution to understanding the origin and evolution of the atmosphere. If the Probe settles into a deposit of aerosols, one needs to extrapolate the accumulated information from the descent measurements to interpret the data. This would offer an opportunity to determine the level of chemical complexity achieved by chemical synthesis in the atmosphere, as even rare aerosols may accumulate in measurable concentrations on the surface. Here the GCMS heated inlet will ensure that the more volatile components of such aerosols reach the instrument. Landing on exposed ice could still permit a measurement of H<sub>2</sub>O ice 'bedrock' and a search for condensed CO<sub>2</sub>, measurements of fundamental importance to an understanding of atmospheric evolution. A determination of D/H in H<sub>2</sub>O on the surface would be of great interest for comparison with atmospheric values in CH<sub>4</sub> and other species. It is recognized, however, that this is the most challenging landing scenario, both for Probe survival and for a good interface between the gas inlet and the surface.

## 2. Instrument Description

### 2.1. GENERAL

Mass spectrometry as the principal chemical identification technique is ideally suited for an exploratory mission like the Huygens Probe and was successfully demonstrated by the Galileo Probe Mass Spectrometer (Niemann, *et al.*, 1996). All atoms and molecules within the mass and sensitivity range of the mass spectrometer will be detected. No a priori knowledge of the composition is required. The simultaneous occurrence of species of similar composition can sometimes lead to ambiguities in species identification. Two electron beam energies in electron impact ionization usually remove the difficulties by generating energy dependent fractionation patterns. Further improvement of species separation and more accurate species identification is achieved with a gas chromatographic system coupled with the mass spectrometer. Gas chromatograph mass spectrometer systems are among the most powerful analytical tools for chemical analysis of many types of compounds, and especially of gas mixtures. The added complexity, compared to stand-alone gas chromatographs or mass spectrometers, is recognized but the benefits resulting from a combined instrument outweigh the possible disadvantage of increased instrument complexity. The advantage offered by combining gas

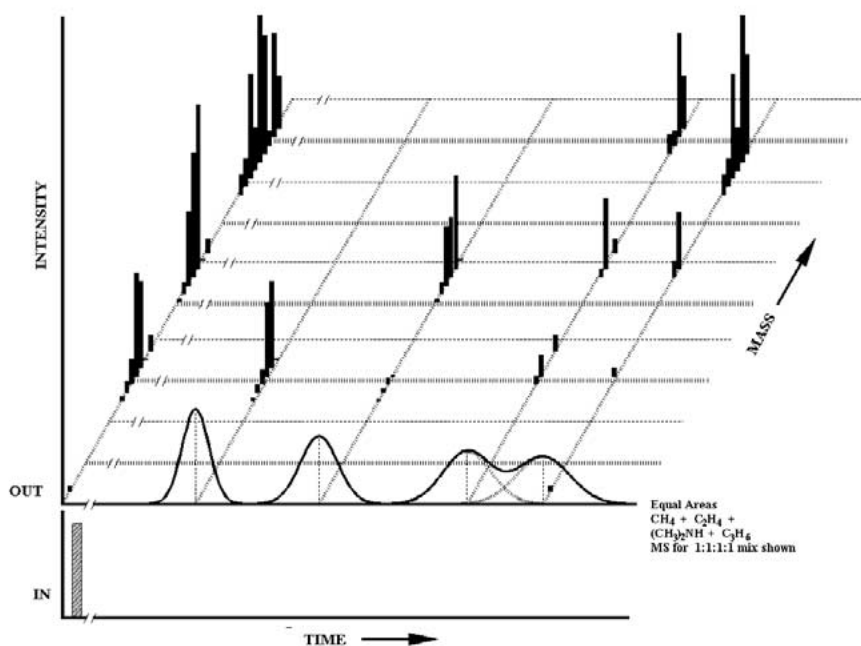


Figure 1. Illustration of the Gas Chromatograph Mass Spectrometer operational principle. Signal intensities are shown in the ordinate vs. time in the abscissa. Column sample injection time is shown in the first trace. The 3D plot shows signal intensities of column elutents for a 4-component sample on the abscissa and the corresponding mass spectra of the elutents in the third coordinate. The simultaneous mass spectra of all four components i.e. without chromatographic separation is shown at the origin and illustrates the significant signal overlap in the mass spectra.

chromatography and mass spectrometry is best illustrated in Figure 1. In this three-dimensional display the detector signal obtained from a gas mixture using only a mass spectrometer vs. mass is plotted at the origin of the time axis, and the detector signal using only a gas chromatograph vs. time is plotted at the origin of the mass axis. The mass spectrum shows a mass overlap at many mass values for the mixture and the gas chromatograph shows distinct peaks without species identification. The advantage of this combination is illustrated in the display allowing time dependent separation of the components by the gas chromatograph and molecular identification of the mass spectrometer.

A functional block diagram showing the main elements of the GCMS/ACP system is shown in Figure 2. The Instrument Operating Characteristics and Huygens Probe Resources Required are summarized below in Table 3 and Table 4.

The main elements of the instrument are:

A mass spectrometer system consisting of ion sources, mass analyzer and ion detector.

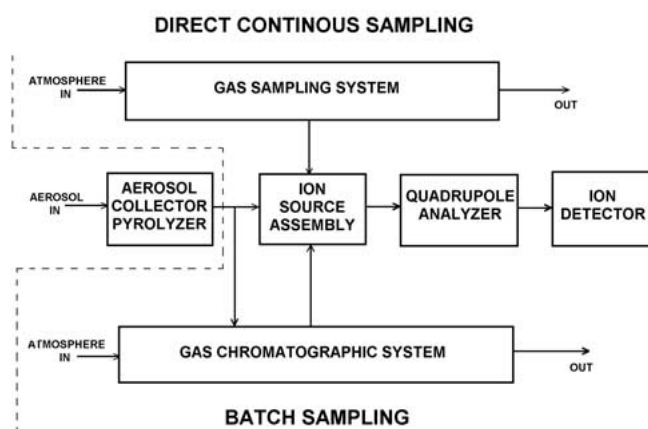


Figure 2. System block diagram of the Gas Chromatograph Mass Spectrometer/Aerosol Collector Pyrolyser showing the major components of the sample collection, processing and mass analyzer subsystems.

A gas sampling system consisting of a direct atmospheric sampling system to introduce atmospheric gas into the ion source and to enrich trace species and noble gases.

A gas chromatograph for batch sampling at specific altitudes in the atmosphere and subsequent time separation of species for identification by the mass spectrometer.

A sample transfer system for gas mixtures, generated by the aerosol pyrolyzer, to the mass spectrometer sample inlet systems. A detailed schematic for the GCMS systems is shown in Figure 3.

The mass spectrometer has five ion sources feeding a common mass analyzer, one ion source at a time. The first source, IS1, samples the atmosphere continuously. The second ion source, IS2, samples the ACP output, and the IS3, IS4 and IS5 ion sources are detectors for three gas chromatographic columns (GC columns). The choice is prescribed for the Probe descent by a preprogrammed sequence.

The ion source connected to the direct atmospheric sample, IS1, is selected during the descent's first 30 min and at any time thereafter when no peaks are present at the output of any of the GC columns. For the analysis of the gas mixture from the ACP, the ion source IS2 will be selected and, during the GC analysis of these mixtures, the sequence will be identical to that associated with the atmospheric GC samples.

TABLE 3  
Instrument operating characteristics

|                         |   |
|-------------------------|---|
| Gas sampling:           | 1) Continuous direct atmospheric gas sampling.<br>2) Batch sampling for GCMS analysis, distributed over descent altitude.<br>3) Sample enrichment for MS (100 to 1000× enrichment). |
| Ambient pressure range: | 1 hPa to 1500 hPa.  |
| Altitude above surface: | 176 km to 0 km.   |
| GC System:              | 3 parallel columns with H <sub>2</sub> carrier gas. Independent MS ion source detection.  |
| Mass analyzer:          | Quadrupole Mass Filter.   |
| Ion source:             | Five sources, electron impact ionization. Maximum operating pressure 1 × 10E-3 hPa.   |
| Ion detector:           | Dual Secondary Electron Multipliers, pulse counting and analog current mode.  |
| Background noise:       | 1 count/min.  |
| Mass range:             | 2 Dalton to 141 Dalton.   |
| Sensitivity:            | 1 × 10E14 counts/s/hPa source pressure.   |
| Dynamic range:          | ≥ 1 × 10E8.   |
| Resolution/crosstalk:   | 1 × 10E-6 for adjacent half mass up to 60 Dalton, less for higher mass.   |

TABLE 4  
Probe resources required

|                        |   |
|------------------------|---|
| Data Rate              | 15 packets per cycle  |
| Viewing requirements:  | 1) Sample inlet near stagnation point.<br>2) Sample outlet near minimum pressure point (e.g. inside of Probe body). |
| Deployment mechanisms: | 1) Metal ceramic breakoff caps, pyrotechnically operated.<br>2) Valves, solenoid operated.                          |
| Altitude information:  | Obtained from altimeter data provided by Probe or ambient pressure desired near surface.                            |
| Temperature range:     | −20 °C to +50 °C operating, −20 °C to +60 storage.  |
| Power:                 | 41 Watts average, 71 Watts peak.  |
| Energy:                | 110 Wh.   |
| I (Max):               | 1.68 A (Main), 1.32 A (Protected).  |
| Weight:                | 17.3 kg.  |
| Size:                  | Cylindrical, 198 mm diameter, 470 mm high. Mounting flange bolt circle 248 mm.                                      |

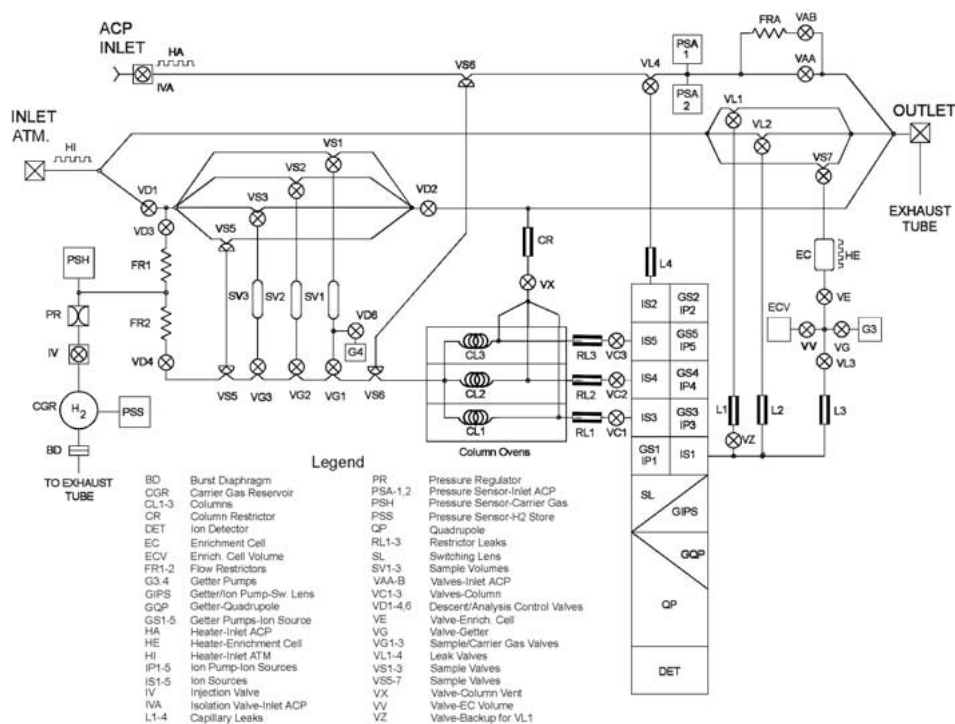


Figure 3. Schematic of the Gas Chromatograph Mass Spectrometer. Details of the Aerosol Collector Pyrolyser are shown in an accompanying paper in this volume.

## 2.2. GAS SAMPLING SYSTEM

The gas sampling system has three subsystems: direct atmospheric sampling, the gas chromatograph and the ACP sample line. The direct atmospheric sampling and the gas chromatograph are self-contained units sharing only the mass spectrometer. The ACP sample line is connected from outside the instrument and interfaces with both the gas chromatograph and the mass spectrometer. The direct atmospheric sampling and gas chromatograph share gas flow lines with a gas inlet port in the Huygens Probe Fore Dome at the Probe apex near the stagnation point and an outlet port at the minimum pressure point at the rear of the Probe. Metal ceramic devices seal inlet and outlet ports. All inlet and outlet lines are evacuated after instrument calibration prior to shipment. They will be opened in sequence by redundant pyrotechnic actuators after Probe entry and ejection of the Probe Front Shield.

### 2.2.1. Direct Atmospheric Sampling

Most of the composition measurements will be obtained from direct atmospheric sampling during descent. Ambient atmospheric gas is conducted through pressure-reducing devices (i.e., leaks) into the ion source, and a sample enrichment and scrubber cell will enhance trace constituent detection and rare gas analysis.

At an altitude of approximately 170 km when the Probe is ready for instrument deployment, i.e. all protective devices are jettisoned, the Atmospheric Inlet and Outlet will be opened to the atmosphere. The inlet port geometry is designed to allow ambient gas to enter from outside of the gas boundary layer. A dynamic pressure of about 70 Pa before parachute jettison and 10 Pa after will force atmospheric gas to flow close to the ion source through the sample system tubulation and manifolds. Small quantities of atmospheric gas will be introduced from the sample system into the ion source IS1 through fixed size leaks and removed at a constant rate by chemical getters and a sputter ion pump. Noble gases will be pumped only by the sputter ion pump and at a slower rate than the reactive gases, increasing the noble gas mixing ratio in the ion source relative to the atmosphere. Laboratory calibration will establish exactly the relationship between ambient and ion source partial pressures.

The gas leaks are arrays of glass capillaries located in the ion source. Typically, seven capillaries per leak are used with inside diameters ranging from 2  $\mu\text{m}$  for the lowest conductance leak to 20  $\mu\text{m}$  for the largest. Capillary arrays instead of single capillaries were chosen in order to reduce the chance of blockage by small aerosol particles. The gas conductances are selected so that the pressure in the ion source does not exceed  $10^{-4}$  hPa in a nominal descent.

The full dynamic range of the mass spectrometer is best used when the ion source pressure is kept at the maximum operating value. Fixed-size leaks do not allow this to occur at all times because the ambient pressure increases during descent. The direct sampling is divided into two sections. This will prevent a large pressure change in the ion source and accommodate a purified noble gas and enrichment cell measurement. A pressure-time profile and measurement sequence are shown in Figure 4. In Figure 4a the change in ambient pressure is shown and predicted cloud or haze levels are also indicated. Nominal values from the Lellouch-Hunten model (Lellouch *et al.*, 1997) of the atmosphere of Titan were used. The pressure variation in ion source IS1 is shown in Figure 4b. From time  $t_0$  to time  $t_1$  leak L1 will be opened by switching the microvalves VL1 and VZ (see schematic Figure 3). While the ambient atmosphere is sampled through leak L1, the enrichment cell EC will be charged. The enrichment cell adsorbs trace gases e.g. high boiling point hydrocarbons and nitriles but no nitrogen or noble gases. By opening valves VS7, VE and VV, gas flows through the cell until the evacuated volume ECV is filled. All remaining reactive gases except methane will then be removed by getter G3 after closing of valves VS7 and VV and opening VG.

The gas flow through leak L1 is discontinued after 30 minutes, at time  $t_1$ , by closing valves VL1 and VZ. The remaining gas in the ion source is pumped out

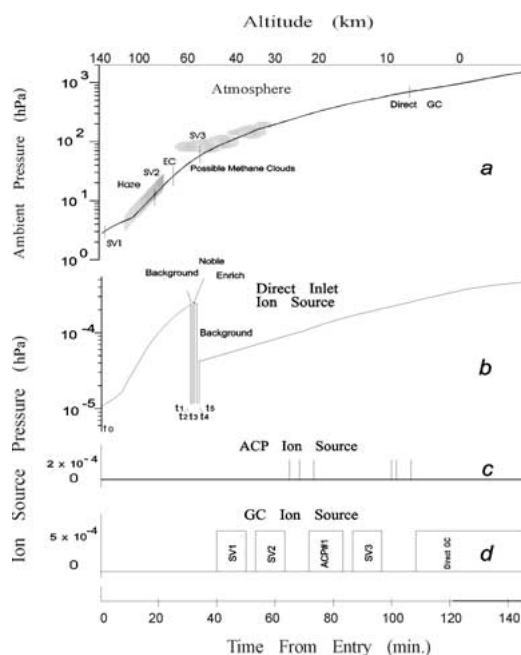


Figure 4. Pressure vs. time profiles of the ambient atmosphere and in the mass spectrometer ion sources during the Probe descent through the Titan's atmosphere. (a) Ambient atmospheric pressure, possible cloud locations and sample enrichment cell and gas chromatograph sample collection times are also indicated. (b) Pressure in the direct sampling ion source. Noble gas and sample enrichment gas analyzer times are: Time  $t_0-t_1$  0–30 mins. Direct atmospheric sampling; Time  $t_1-t_2$  30–31:29 mins. Background; Time  $t_2-t_3$  31:29–33:00 Rare gas cell; Time  $t_3-t_4$  33:00–34:50 Rare gas and enrichment cells; Time  $t_4-t_5$  34:50–36:00 Instrument background. (c) ACP ion source dedicated sampling time. (d) Operating times of the three ion sources dedicated to the gas chromatographic columns.

leaving only background pressure which will be measured by the mass spectrometer. At time  $t_2$  the enrichment cell will be isolated by closing valve VE and heated to desorb the collected trace gases. Simultaneously, the gas mixture residing between the valves VV, VE, VG and VL3 will be introduced into the ion source IS1 through L3 for noble gas analysis. At time  $t_3$  the gas content of the enrichment cell will be added to the gas mixture for analysis by opening valve VE. When the enrichment cell and noble gas analysis are complete at time  $t_4$ , the subsystem will be isolated from the ion source by closing valve VL3 and background pressure is observed again. At time  $t_5$ , 36 minutes, direct leak L2 will be activated by opening VL2 until the end of the mission. Sampling for the first 30 minutes through leak L1 will be continuous and at a high rate. The direct atmospheric sampling through leak L2 will be interrupted repeatedly by sampling sequences for the analysis of elutents from the gas chromatographic columns and ACP products.

### 2.2.2. Gas Chromatographic Analysis

Gas chromatography allows, under suitable conditions, the gas phase separation of complex mixtures of hydrocarbons, nitriles and permanent gases including carbon monoxide. This technique has already been used successfully in planetary exploration (Raulin *et al.*, 1992b).

A small amount of an unknown mixture of gases is introduced into a carrier gas stream which flows continuously into a specially prepared gas chromatograph column. Each component in the mixture, in the ideal case, elutes from the column outlet at a different time. A detector at the outlet gives a signal related to the quantity or concentration of the components of the gas mixture.

Difficulties in data interpretation result when universal detectors are used because the exact chemical composition of the eluent is not known. A mass spectrometer eliminates most of the difficulties (see illustration in Figure 1). Advantages and disadvantages of combined GCMS instrument techniques have been discussed in great detail in the technical literature (Watson, 1997; Kitson *et al.*, 1996; McFadden, 1973); and the arguments apply to this application as well. One disadvantage is the increased complexity of the instrument which must be of particular concern here because of the specific mission environment. The short time available for sampling and analysis, long time reliability and severe limits placed on weight and power require special considerations.

The use of open capillary columns (Do and Raulin, 1989, 1990, 1992; de Vanssay *et al.*, 1993; Aflalaye *et al.*, 1995) and of packed columns (de Vanssay *et al.*, 1994) were considered. Best instrument performance and moderate instrument complexity have to be balanced in this design. Three chromatographic columns with different properties are used and operated in parallel to cover the range of expected atmospheric species (Navale *et al.*, 1998). One column will separate CO and N<sub>2</sub> and other stable gases. A second column will separate nitriles and other organics with up to three carbon atoms. A third column will provide the separation of C<sub>3</sub> through C<sub>8</sub> saturated and unsaturated hydrocarbons and nitriles of up to C<sub>4</sub>. A silica steel micropacked GC column 2 m in length with 0.75 mm internal diameter (for column 1) and silica steel wall coated open tubular (WCOT) GC capillary columns 10 m and 14 m in length with 0.18 mm internal diameter, (for columns 2 and 3) were found to be most suitable. The columns are wound in a 178 mm diameter coil on high temperature foil heaters. A thermally isolated oven encloses each column to allow efficient heating. The columns will be operated at 0.18 MPa inlet pressure and the outlet is vented through a flow restrictor to the ambient atmosphere.

Hydrogen was selected as carrier gas because of efficient storage and pumping. It is stored in 100 g of hydride metal alloy enclosed in a stainless steel housing. The amount of hydrogen required for the GC operation, assuming 180 minutes descent time and a 50% reserve, is approximately 3 standard liters. The hydrogen carrier gas reservoir (CGR) will be equipped with an injection valve IV shown schematically in Figure 3. The valve is solenoid operated and similar in design to



the microvalves. The valve plunger punctures a diaphragm and initiates carrier gas flow. A miniaturized silicon diaphragm pressure sensor, PSH, is used to monitor the pressure in the CGR. A pressure regulator, PR, controls the flow through the flow restrictors and columns. For safety a burst diaphragm, BP, installed in the CGR is set to burst at 3 MPa.

The Probe does not spend sufficient time for repeated gas chromatographic analysis in the altitude region between 176 km and 60 km. To overcome this difficulty samples will be collected at specified times during the descent through this region of the atmosphere in sample volumes SV1 through SV3 for later analysis. In the lower atmosphere and near the surface, samples will be injected directly from the atmosphere into the carrier gas flow path of the GC.

At system initiation hydrogen carrier gas flows from the hydrogen reservoir CGR (see Figure 3), through the injection valve IV, pressure regulator PR, restrictor FR2 and valve VD4. After passing through sample injection valves VS5, VG1, 2, 3, the gas flow splits into the three GC columns. A fraction of the flow exiting the columns will be split off and conducted through capillary leak arrays, RL1, 2 and 3, into the ion sources. The remaining gas will be vented through valve VX and column restrictor CR.

The atmospheric samples collected in the sample volumes will be analyzed one at a time by first flushing the inlet manifold between valves VD1 and VD2 with carrier gas and then operating valve pairs VS1, VG1, etc. several milliseconds to allow the sample volume to be discharged into the carrier gas stream. The GC analysis time allowed per sample is about 10 minutes. Direct sample injection will be accomplished in a similar fashion by first closing VD1 and VD2 and injecting part of the trapped sample gas through valve VS5 by redirecting the carrier gas flow through VD3 for a short time interval. Injection of the ACP sample from the sample transfer manifold into the GC column will be accomplished through valve VS6 in a similar manner. A time profile of the complete GC sampling sequence is shown in Figure 4d.

### 2.3. AEROSOL COLLECTOR PYROLYSER ANALYSIS

The operation of the Aerosol Collector Pyrolyser (ACP) and details of the sample transfer are described in a separate paper (see Israel *et al.*, this volume). The pyrolysis products will be provided through a sample transfer line made of 0.5 mm internal diameter nickel tube connected to an injection valve IVA (ACP Inlet in Figure 3) at the center of the instrument housing. Internally a feed tube connects to the GC inlet valve VS6, the direct inlet valve VL4 and to the outlet via valves VAA, VAB, and flow restrictor FRA.

The ACP line will be opened just prior to the first sample transfer. When gas flow has been established, sample gas analysis begins using the dedicated ion source IS2. After analysis is completed, sample gas in the ACP line is vented through the outlet and the line is refilled with the next sample. The sample for

the gas chromatograph is injected by opening valve VS6 for a short time interval to superimpose the sample on the carrier gas stream as described in the previous section. The time line for the ACP sampling is shown in Figure 4c.

#### 2.4. POST SURFACE IMPACT ANALYSIS

It is likely that the Probe will continue to operate for a short time after surface impact. As the nature of the surface is not known, it is hard to predict the specific contact the Probe will make. The most probable landing position is expected to be upright, which is also optimum for the instrument. In case of a landing on a liquid surface, the heated inlet tube will be submerged in the liquid, which will rapidly evaporate in the inlet tube and the vapors will flow through the inlet lines. Rapid direct sampling through leak L2 will provide composition measurements of the vapor. In case of a landing on a solid surface, the surface will be heated locally by the inlet tube and volatized gases will flow through the inlet lines and be available for analysis.

GC analysis will be initiated through valve VS5, as described above, if the Probe survives for more than two minutes.

The surface sampling mode will be initiated by an altimeter signal shortly before surface impact.

#### 2.5. ION SOURCES

Electron impact ionization is used in the miniaturized ion sources. A well collimated electron beam is directed through the ionization region into which the gas stream is conducted by the capillary leaks. The flow paths are short because the valves and capillary leaks are mounted directly on the ion sources. The electron guns have heated filaments of 0.075 mm diameter (97% tungsten, 3% rhenium) wire and require approximately 1 watt of power. The electron beam energies can be chosen from two pre-selected values (i.e., 25 eV or 70 eV) to permit species identification and discrimination by observing energy dependent fractionation. A typical electron beam current is 80  $\mu\text{A}$ . Ions are focused and transmitted into a quadrupole switching lens assembly by multi-element ion lenses of small aperture. Quadrupole switching lenses are operated as ion beam deflectors. Any one of the five ion beams can be deflected by the switching lens into the quadrupole mass analyzer at any time. Switching is accomplished in microseconds by changing the bias voltages to the appropriate values for the ion source of choice. The ion source arrangement and the switching lens system are shown schematically in Figure 5a.

Sample gas decoupling of the ionization regions is achieved by differential pumping. The principle of sample decoupling is shown in a schematic diagram in Figure 5b. By designing the gas conductances  $C$  such that their ratios  $C_1/C_2$  and  $C_1/C_3$  are approximately  $10^3$  and  $10^2$  respectively, the separation in partial pressures between ionization regions is  $10^6$ . For example, gas in ion source IS1 with a partial pressure of  $10^{-6}$  hPa will be seen by the other ion sources as a partial

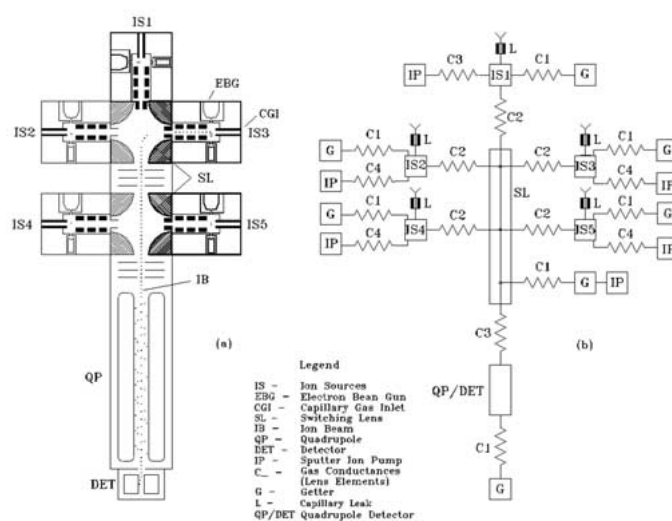


Figure 5. Illustrations of ion source configuration and schematic of differential vacuum pumping system.

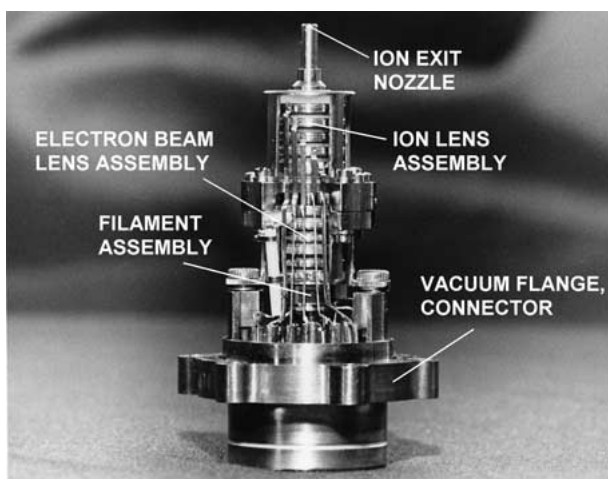


Figure 6. An ion source showing the electron and ion focusing lenses. The overall height is 63 mm.

pressure of  $10^{-12}$  hPa. The pressure in the quadrupole mass filter and detector region is below  $10^{-6}$  hPa to eliminate ion scattering. The size of conductances  $C_2$  is determined by the ion lens apertures which are designed to be long and narrow. The pumping speed of the getters and the sputter ion pumps determine the size of conductances  $C_1$  and  $C_4$ . An ion source, showing the electron and ion lens arrangement and an ion source system showing the individual ion source and the switching lenses in the partially assembled ion source housing are seen in the photograph in Figure 6 and Figure 7, respectively.

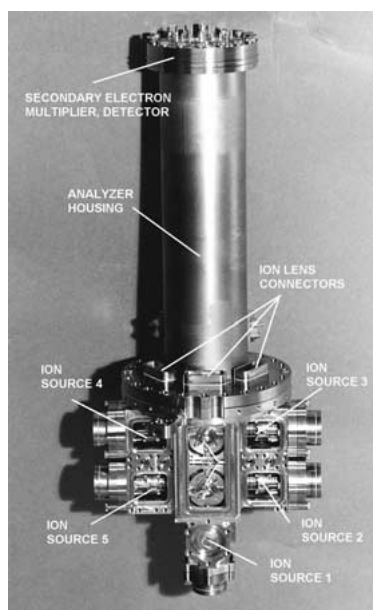


Figure 7. The ion source system, showing the individual ion sources and the switching lenses in the partially assembled ion source housing before installation of the getter housings and the gas inlet manifolds. The overall length is 357 mm.

## 2.6. QUADRUPOLE MASS FILTER AND ION DETECTOR

The quadrupole mass filter accepts the ion beam generated by the ion sources transmitting only ions of a chosen charge to mass ratio. Detailed descriptions of the operating principle of quadrupole mass filters can be found in the technical literature (e.g., Dawson, 1976). The selected ion beams are focused on two secondary electron multiplier ion detectors. The quadrupole rods are excited by radio frequency ( $V_{AC}$ ) and direct current ( $V_{DC}$ ) potentials which together create a dynamic electric field within the quadrupole region that controls the transmitted mass ( $m/e$  value) and the resolution. A mass scan is executed by varying the radio frequency potential  $V_{AC}$  to satisfy the relationship  $M = 0.55 V_{AC}/f^2$  where  $V_{AC}$  is in volts,  $f$  in MHz, and  $M$  in Dalton. The resolution will be controlled over the mass range (2–141 Dalton) by programming the ratio of  $V_{DC}$  to  $V_{AC}$  to maintain the resolving power defined by a crosstalk criterion appropriate for that mass range. The ion transmission efficiency will be 100% resulting in flat top mass peaks over the mass range of interest. This allows a mass scan mode in which each mass is monitored by a single step.

In another operating mode, the DC voltage will be reduced to zero which creates a high pass filter giving the sum of all masses greater than, for example, 2 Dalton. This feature allows the use of the mass spectrometer as a nonspecific GC-detector

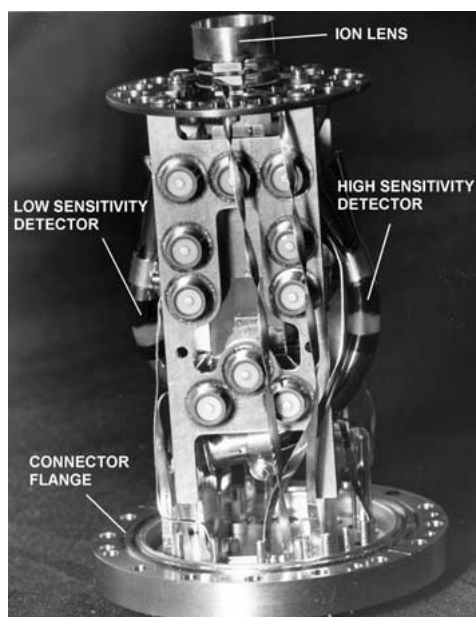


Figure 8. The ion detector assembly, showing the entrance lenses, the support structure, and the location of the continuous channel secondary electron multipliers. The overall length is 110 mm.

excluding the detection of the abundant hydrogen ions produced by the GC carrier gas.

The ions passing the mass filter will be detected by a pair of continuous dynode secondary electron multipliers with effective entrance aperture sizes differing by a factor of  $3 \times 10^3$ . Charge pulses at the anodes of the secondary electron multipliers are amplified and counted. The background noise of the secondary electron multipliers is approximately one count per minute. The upper count rate is limited to approximately  $3 \times 10^7$  counts/s by the pulse width of the anode pulses of the secondary electron multipliers. The instrument sensitivity for 100% ion transmission is approximately  $1 \times 10^{14}$  counts per sec per hPa. Secondary electron multiplier background count rates of one count per minute or less yields a detection threshold of  $1.7 \times 10^{-16}$  hPa partial pressure in the ion source region for a signal to background count ratio of unity. The maximum pressure level in the ionization region is limited by mean free path conditions to about  $10^{-3}$  hPa. In the low mass range ( $<46$  Dalton) the lower detection limit is often not realizable because of background gases emitted from the surrounding surfaces or because of interference at some mass numbers from other gases present in high concentrations. Typical background gases in the ion source are  $\text{H}_2$ ,  $\text{CH}_4$ ,  $\text{H}_2\text{O}$ ,  $\text{CO}$ , and  $\text{CO}_2$ . The exact sensitivity is established by calibration and varies with species because of differing ionization efficiencies for neutrals and the conversion efficiency at the secondary electron multiplier. The detector assembly, consisting of the entrance

lenses, support structure and the continuous channel secondary electron multiplier, is shown in Figure 8.

## 2.7. PUMPING SYSTEMS

The pumps establish a flow of sample gas through the ion sources when a sampling device is opened. They remove the gas from the ion source regions after analysis and closure. Non-evaporable getters and sputter ion pumps are used because they are easily adapted to space flight systems. The sputter ion pumps depend only on electrical power for operation and work without moving parts. Hydrogen is sorbed reversibly at a very high rate and in very large quantities by the getter material, while nitrogen is efficiently pumped by irreversible bonding. The getter material is sintered titanium and molybdenum powder. The sorption capacity for hydrogen is  $\sim 20$  hPa liter/g for an equilibrium pressure of  $10^{-4}$  hPa at a worst case temperature of  $200^\circ\text{C}$ . More favorable conditions exist at the expected operating temperature of  $<100^\circ\text{C}$ . The getters, after activation in a vacuum, will remain activated indefinitely at room temperature. The components of a getter pump assembly consisting of the getter wafers, heat shields and the housing are shown in Figure 9.

Uncertainties exist about the concentration of argon and methane in Titan's atmosphere. These gases will be pumped by sputter ion pumps. Synthesis of hydrocarbons in the sputter ion pumps is minimized by special processing of the cathodes. A partially assembled sputter ion pump, the anode, cathode and housing without magnet assembly, is shown in Figure 10.

## 2.8. ELECTRONIC SYSTEM

The electronics system block diagram is shown in Figure 11. The various subsystems required to control the sample flow, to power the sensor and ion detectors and process the output signal are under control of a microcomputer. Instrument potentials are produced by a number of programmable, floating-secondary DC-DC converters that are configured for each measurement. Telemetry and command streams connect to the spacecraft through redundant serial interfaces. The electronics system provides the flexibility to accommodate the diverse measurement and testing requirements.

The pyrotechnic devices used to break the ceramic seal in the sample inlet and outlet systems are fired by the Probe pyro bus. The sample-sequencing microvalves are powered by switching circuits under microcomputer control. Each of the five ion source supplies contains a filament emission regulator and electrode supply to provide the required voltages and currents. Fast switching of the ion beam deflectors is accomplished by high-speed bipolar electronic switches.

The quadrupole  $V_{AC}$  and  $V_{DC}$  potentials are generated in a dedicated supply. Prior to each measurement the microcomputer calculates the proper amplitudes and frequency step for the  $V_{AC}$  potential. An auto-tune algorithm is incorporated

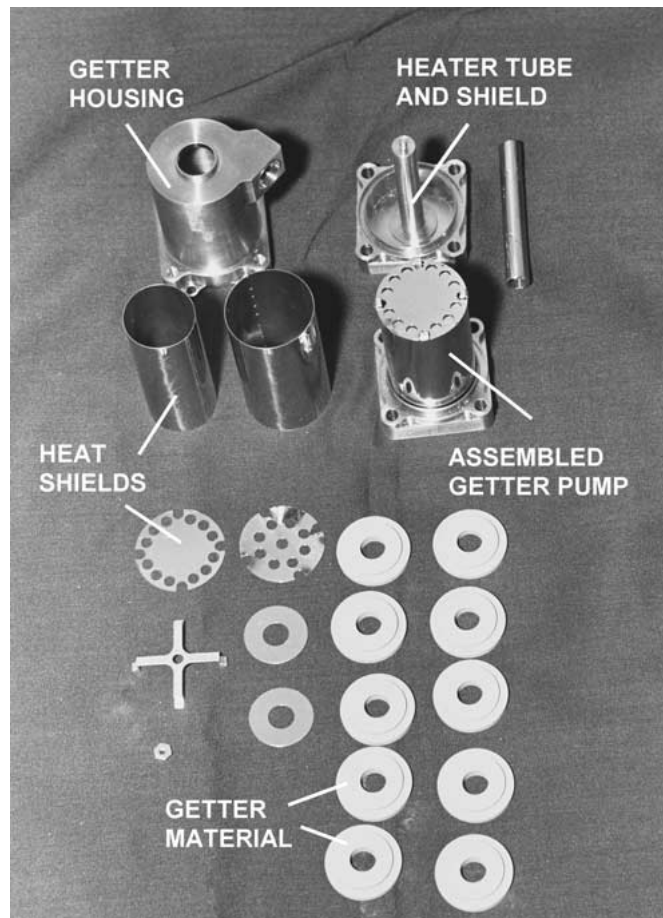


Figure 9. Components of a getter pump assembly consisting of getter wafers, heat shields and housing. The wafer diameter is 25 mm.

into the control software to assure that changes such as component aging in the supply do not affect mass tuning and resolution.

Current pulses from the secondary electron multiplier are amplified by a low-noise trans-resistance amplifier and counted. The counts are held in a 32-bit register, which is then read by the microcomputer. A parallel electrometer channel measures multiplier current when the maximum count rate is approached allowing an inflight gain check.

A 1750A microprocessor controls and sequences the instrument in accordance with software instructions contained in programmable read-only memory (PROM). Control of the many subsystems is accomplished by writing to a separate, high-speed sensor data bus. The instrument software was written in a high-level language (i.e., Ada) whenever possible and in assembly language when speed is crucial. Code has been developed in a modular, top-down manner to increase test-

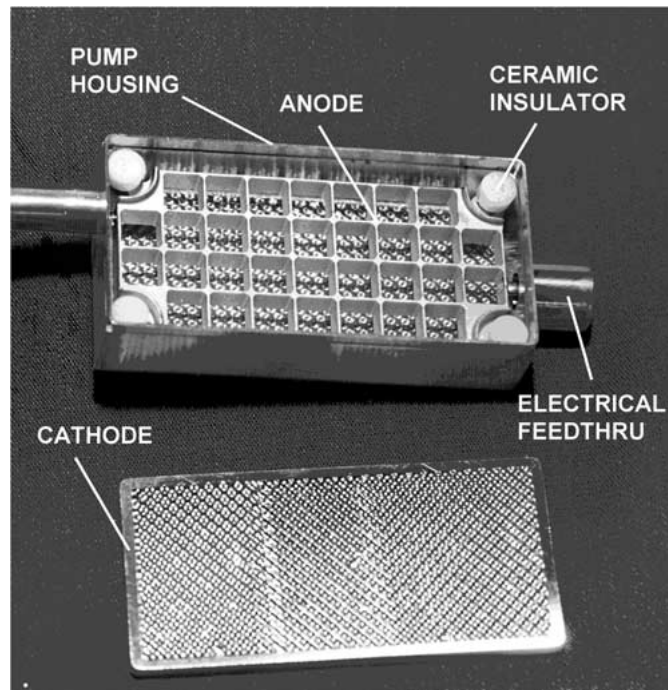


Figure 10. A partially assembled sputter ion pump, showing the anode grid structure, the cathode and the housing. (Indicated dimensions are in inches).

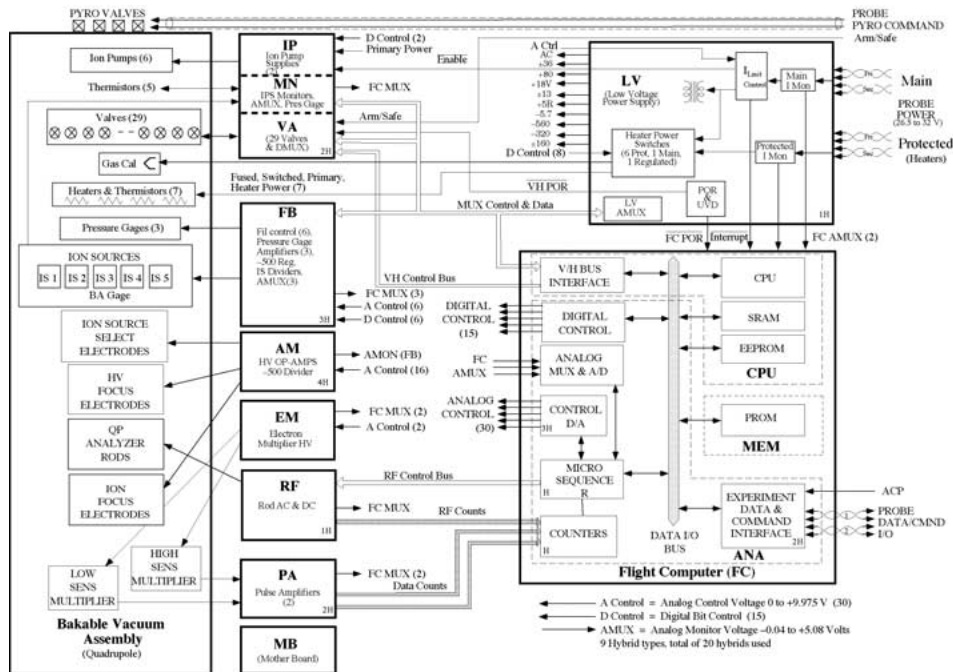


Figure 11. Electronics block diagram showing major digital and analog circuit subsystems.



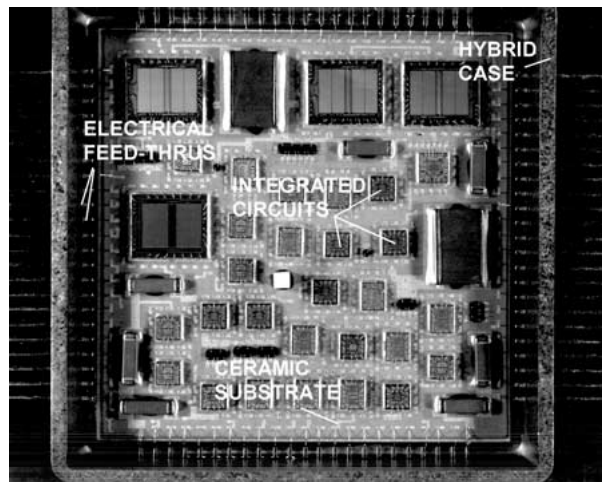


Figure 12. An unsealed electronics circuit packaged in hybrid form. The circuit is the microsequencer subsystem. Side dimension is 57 mm.

ability and improve maintainability. The instrument will receive commands and transmit science and housekeeping data through the Probe Command and Data Management System (CDMS) interfaces.

Power to the instrument is derived from the common +28 V spacecraft bus. Inrush current limiting and overload protection is provided in the main power converter. The spacecraft bus voltage is transformed by a DC-DC converter to a number of standard secondary potentials that power the subsystems. To minimize size and weight of the electronics system approximately 80% of the electronic circuits are packaged in hybrids. A typical hybrid circuit, the micro-sequencer, is shown in Figure 12.

## 2.9. MECHANICAL CONFIGURATION

The mechanical layout of the instrument is shown in Figures 13 and 14. The ion source and mass analyzer assembly constitute the main body of the sensor system. Getter pumps and sputter ion pumps are directly mounted to the ion sources at the upper part of the assembly for compactness. The GC columns and the gas sampling system are concentrically arranged around the ion source assembly. The gas inlet tube, shown in Figure 13, extends forward to penetrate through the fore dome. The electronics system is located below the gas sampling system. The electronics support structure and the electronic circuit boards are shown in Figure 14. The electronics support structure is made of aluminum alloy and is attached to the center section of the instrument housing.

The instrument housing is also made of aluminum alloy and consists of three sections as shown in Figure 15. The lower housing encloses the sampling system and the ion sources. It also provides the inlet port interface with the fore dome of

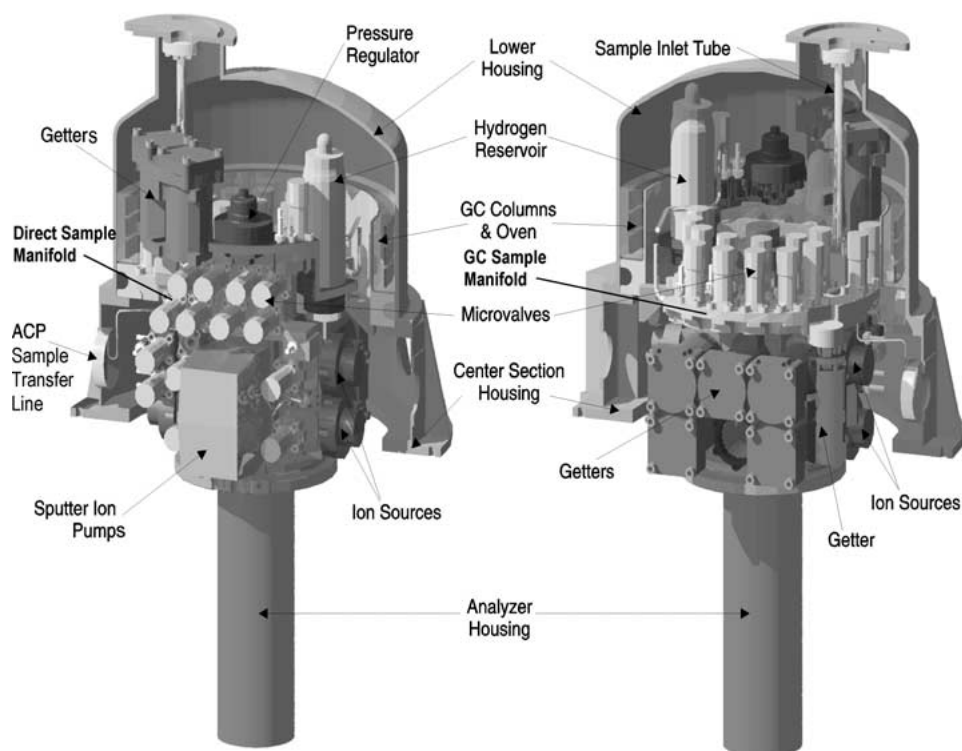


Figure 13. Computer-generated cutaway views of the Gas Chromatograph Mass Spectrometer, gas sampling, mass analyzer and vacuum pumping systems.

the Probe. The upper housing covers the electronics system. The center housing provides the mounting support for all instrument components and most external interfaces. The housing is hermetically sealed by metal seals. The overall helium leak rates of  $<10^{-8}$  hPa l s $^{-1}$  is sufficient to maintain the housing pressurized for more than ten years. The housing is designed to withstand 0.15 MPa internal pressurization and an external pressure of 0.15 MPa above the internal pressure. For flight, the housing is filled with dry nitrogen to 0.12 MPa.

The instrument is mounted on the Experiment Platform of the Probe (see Lebreton *et al.*, Figure 10, this issue) via a flange at the center housing. The sample inlet line penetrates the Probe fore dome (see Lebreton *et al.*, Figure 11, this issue) near the stagnation point outside of the boundary layer of the gas flow around the Probe body. The sample outlet port is at the rear section of the housing. The mounting position of the Aerosol Collector Pyrolyser on the Experiment Platform is adjacent to the GCMS for efficient sample transfer.

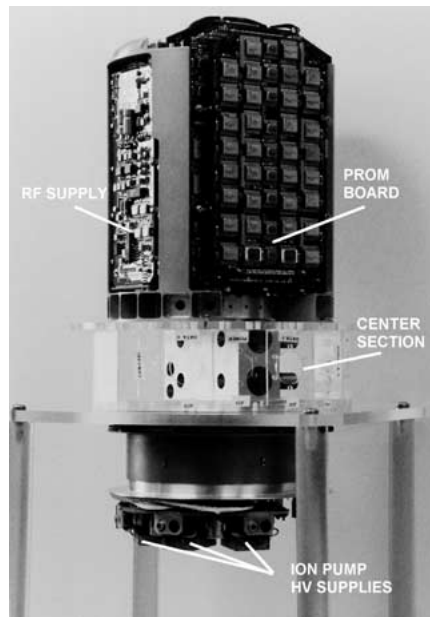


Figure 14. The assembled electronics package and support structure. Shown in front is the Programmable Read-Only Memory (PROM) board.

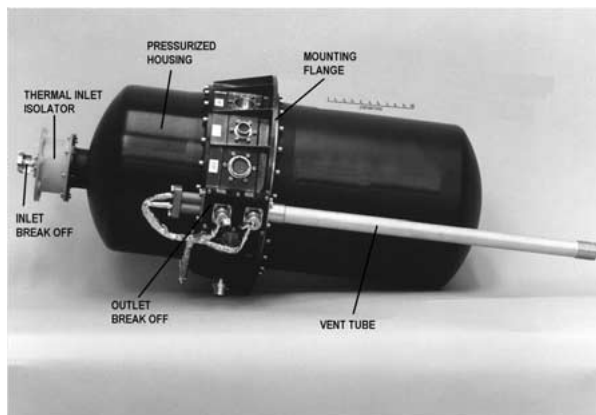


Figure 15. The assembled GCMS. The lower housing encloses the sampling system and the ion sources, while the upper housing covers the electronics system. The gas inlet port is at the dome of the lower housing. The sample gas is vented through a fiberglass tube toward the rear of the Probe. The housing is hermetically sealed and pressurized to 0.12 MPa during flight. (Indicated dimensions are in cm).

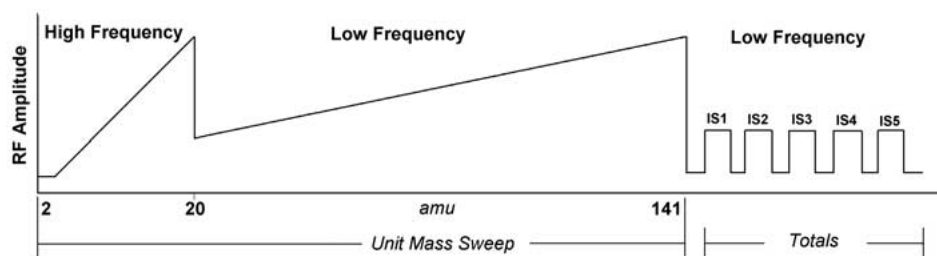


Figure 16. Illustration of a 'Full Scan' of the mass analyzer from 2 to 141 Dalton.

#### 2.10. SAMPLING STRATEGY

Throughout the entire descent of the Huygens Probe through the atmosphere of Titan, the GCMS will perform a single charge to mass ratio measurement each 5 ms. A full scan will be performed each 936.5 ms selected from one of the five ion sources. The mass range measured with each ion source is determined by a stored sequence. The sequence also determines which ion sources are enabled for sampling during various stages of the descent. The sequence of measurements is shown in Figure 4. During the first 36 minutes of the descent, the direct inlet into a mass spectrometer ion source is analyzed, and atmospheric samples are collected for subsequent analysis by the GCMS. During the same interval, an atmospheric sample is processed to enrich the noble gas content to extend the sensitivity of the noble gas ratio analysis. During the descent interval between 40 and 95 minutes, the collected samples are analyzed sequentially by the GCMS as indicated in Figure 4, panel d. The output of the ACP is analyzed both directly by the MS and by the GCMS during intervening periods. In each of these analyses, the characteristics of the mass scan can be programmed.

Each integral mass number from 2 to 141 Dalton is sampled sequentially. During all mass scans, the total output from each ion source (with carrier gas rejected) will be measured. The purpose is to provide a continuous record of the total density in each ion source and to select the ion source to be sampled when an unknown gas mixture is flowing through the gas chromatographic columns. An illustration of the Full Scan is shown in Figure 16.

For the direct mass spectrometer measurements, 936.5 ms are required to complete a Full Scan. This resolution is more than adequate to define the atmospheric profile defined by the descent rate and will be used. The operation of the instrument when three GC columns are simultaneously on range is shown in Figure 17.

A diagnostic scan of the full mass range in 1/8 Dalton increments will be made at times during the descent when the rate of change of the atmospheric samples is lowest. This diagnostic scan and others will be interleaved with the atmospheric measurements.

The output of the Aerosol Collector Pyrolyser (ACP) will be sampled both directly and through the GC columns at the appropriate time in the descent as outlined

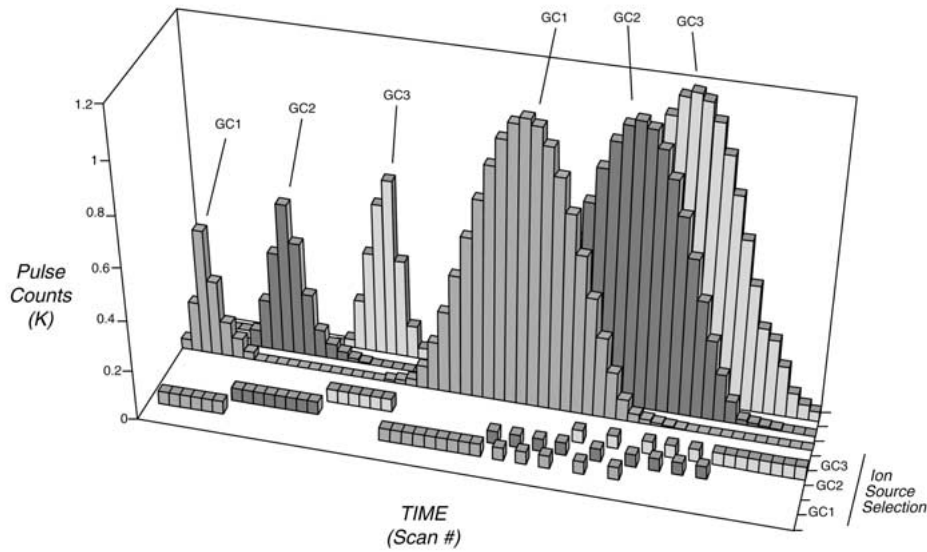


Figure 17. An illustration of the operation of the instrument when three GC columns are simultaneously on range.

in the accompanying paper describing the ACP and its operation. The same mass scan capabilities available for the GCMS measurements are available to the ACP instrument.

## 2.11. DATA FORMAT

The GCMS is intrinsically capable of generating much more data than can be transmitted within the bandwidth allocated to the instrument. Counter data are produced as two 16-bit words each integration period, one from the high sensitivity and one from the low sensitivity secondary electron multiplier. Only data from one counter are selected for telemetry. The data are compressed by taking the square root of the counter contents when the pulse count rate is  $\geq 2.56 \times 10^4$  per second to yield 8 bits of counter data per integration period with one bit added for counter identification.

Even with data compression, science and housekeeping data are produced at approximately twice the available rate of a single telemetry channel assigned to the instrument. For this reason, the data will be sent alternately to the two (redundant) channels. If both telemetry channels function, all data will be recovered. If one channel fails, the effect will be to reduce the temporal resolution of the science data.

The science and housekeeping data are configured as subpackets within the standard Huygens Probe telemetry packet. The GCMS is allotted 15 telemetry packets per 16-second cycle; each packet is 126 octets in length, but seven of those

are reserved for packet header and error correction. This results in an actual data rate available to the GCMS of 885 bits per second per channel.

**Science Data Subpacket:** Data from one mass scan are packetized along with time tag information and are sent to telemetry once every 936.5 msec. These subpackets contain 1488 bits, for a data rate of 1589 bits per second.

**Housekeeping Data Subpackets:** Three different subpackets are used for low, medium, and high-speed housekeeping data. The total of the three types is approximately 100 bits per second.

**Acknowledge Subpackets:** These are used to send confirmation of external events such as ACP sync pulses and telecommands. Each subpacket consists of 32 bits.

Subpacket synchronization and descent sequence monitoring data consume an additional 52 bits per second (for both channels). This results in a total GCMS data production rate of approximately 1741 bits per second, versus the available telemetry of 1770 bits per second for two channels used alternately. If the Probe retrieves data faster than science data are being produced, the GCMS will insert idle subpackets which contain housekeeping data.

### 3. Instrument Calibration

In order to determine the overall system transfer characteristics, the instrument was calibrated on a dynamic flow system where the time, pressure and temperature profile to be encountered during the Probe descent was simulated. Gas mixtures containing known mixing ratios of gases were introduced into the high pressure flow system of the sample inlet system of the flight instrument. The design of the sample inlet system allows instrument calibration as it is used in flight. Components with limited operational lifetime i.e. getter materials and the sputter ion pumps were replaced after calibration. All pumps are designed to operate in a conductance limited mode so that small changes in pump performance will have a negligible effect on the instrument transfer function.

The calibration system consists of two parts: the high pressure gas flow and sample mixing system and the ultra high vacuum pumping stand. The high pressure gas flow and sample mixing system allow for the preparation and introduction into the unit of known gas mixtures at representative pressures and temperatures.

The ultra-high vacuum pumping stand is used to evacuate the ion sources, analyzer, detector, sample inlet system and the gas chromatograph subsystems. It is needed for the calibration (i.e., bakeout, getter activation) and tests of the instrument and also for final processing before pinch off. To assure isolation of each subsystem from the others, each subsystem requires its own pumping system, i.e., each ion source, the analyzer and detector subsystem, the direct sampling GC and enrichment cells were connected to separate pumping stations. During calibration the pumping station could be isolated from the instrument by bakable, miniature, ultra high vacuum valves.

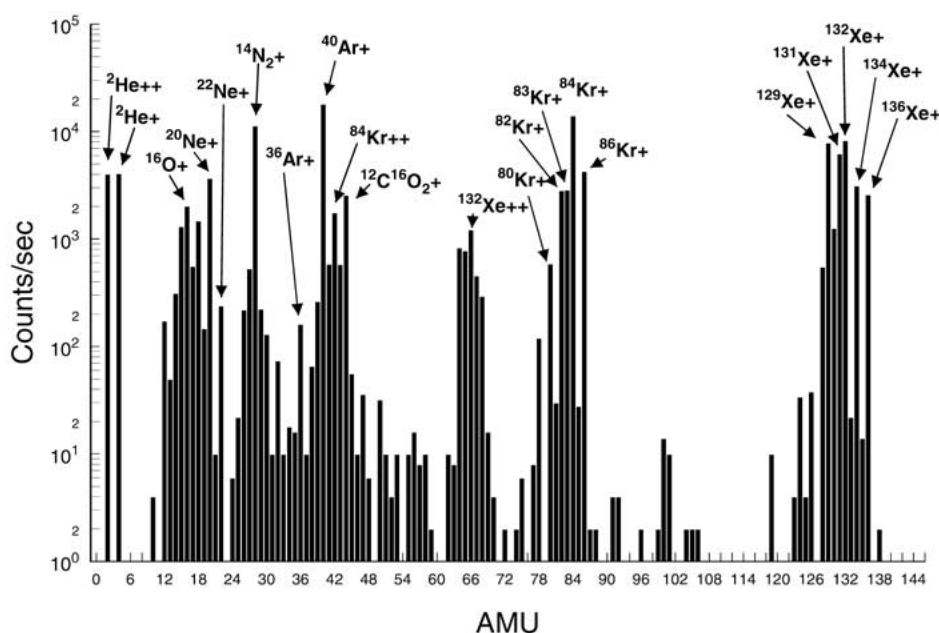


Figure 18. MS spectrum from 1–144 Daltons during characterization of the GCMS in the laboratory.

A complete MS spectrum from 1–144 Daltons recorded during characterization is shown (Figure 18). A noble gas mixture listed in Table 5 was used for this sample.

A schematic diagram of the calibration system is shown in Figure 19. The flight instrument inlet and outlet ports are connected directly with vacuum flanges to the appropriate terminals of the high pressure gas flow system. The flow lines were thermally isolated and the gas temperature was controlled by heaters and heat exchangers. Absolute system pressure and the differential pressure across the inlet were monitored with precision pressure gauges. The gas flow was adjusted so that the differential pressure was equal to the Probe stagnation pressure expected in flight. Trace gas mixtures were added through the calibration gas line or they were introduced from prepared gas tanks with certified mixing ratios. The exact quantity of added calibration gas was determined by measuring the gas flow with flow meters and the pressure at the injection port.

Following the instrument measurement sequence, gas mixtures were introduced into the respective ion source and the GC subsystem at the appropriate times and pressure level consistent with the expected descent pressure and time profile. The separate ACP-GCMS compatibility test was performed to assure proper timing and sample transfer.

## GCMS Calibration System

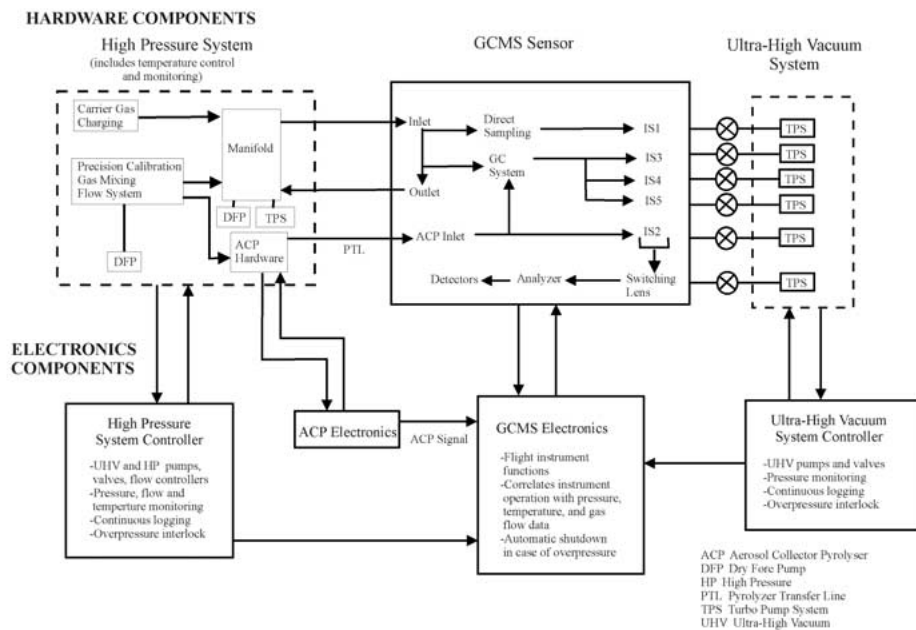


Figure 19. Schematic diagram of the calibration system.

### 3.1. GAS MIXTURES USED IN GCMS SENSOR CHARACTERIZATION

In addition to the pure gases used for initial characterization, i.e.,  $N_2$ ,  $CH_4$ ,  $H_2$ , Table 5 gives the certified gas mixtures that were utilized during the final calibration of the GCMS.

### 3.2. POST-LAUNCH CALIBRATION

The GCMS Flight Spare model together with the ACP Flight Spare model will be calibrated prior to Titan encounter following the same process as was used for the Flight Units. Since more time will be available, additional calibration gas mixtures will also be considered. Finally, the spare instruments and the calibration facility will be maintained and prepared for post encounter calibration and laboratory reproduction of the flight data in order to aid in the interpretation of the flight data.

## 4. Post Launch Performance and Testing

A full post-launch checkout of the GCMS was performed on 23 October 1997. Subsequent checkouts were performed approximately every six months. The operation was completely nominal in all cases. All housekeeping data and science data



TABLE 5  
Calibration gas mixtures

---

a. Nitrogen(N<sub>2</sub>) mixture with trace amounts of various light hydrocarbons and other components:  
~100 ppm each of

|   |   |   |
|---|---|---|
| methane (CH <sub>4</sub> )                    | ethane (C <sub>2</sub> H <sub>6</sub> )       | ethene (C <sub>2</sub> H <sub>4</sub> )   |
| ethyne (C <sub>2</sub> H <sub>2</sub> )       | propane (C <sub>3</sub> H <sub>8</sub> )      | propene (C <sub>3</sub> H <sub>6</sub> )  |
| nbutane (C <sub>4</sub> H <sub>10</sub> )     | cis2butene (C <sub>4</sub> H <sub>8</sub> )   | 1butene (C <sub>4</sub> H <sub>8</sub> )  |
| trans2butene (C <sub>4</sub> H <sub>8</sub> ) | 1,3butadiene (C <sub>4</sub> H <sub>6</sub> ) | pentane (C <sub>5</sub> H <sub>12</sub> ) |
| carbon dioxide (CO <sub>2</sub> )             | carbon monoxide (CO)                          | pentene (C <sub>5</sub> H <sub>10</sub> ) |

b. Nitrogen(N<sub>2</sub>) mixture with trace amounts of various heavy hydrocarbons:  
~100 ppm each of

|  |   |  |
|--|---|--|
| 2methylpropane (C <sub>4</sub> H <sub>10</sub> ) | 2methylbutane(C <sub>5</sub> H <sub>12</sub> )        | isohexane(C <sub>6</sub> H <sub>14</sub> ) |
| benzene (C <sub>6</sub> H <sub>6</sub> )         | toluene (C <sub>7</sub> H <sub>8</sub> )              | oxylene (C <sub>8</sub> H <sub>10</sub> )  |
| 3methyl,1butene                                  | 2,2dimethyl propane (C <sub>5</sub> H <sub>12</sub> ) |  |

c. Nitrogen(N<sub>2</sub>) mixture with trace amounts of various noble gases:  
~50 ppm each of xenon, krypton, argon  
~250 ppm neon                      ~575 ppm helium

d. Nitrogen (N<sub>2</sub>) with 10% argon

e. Helium with ~1000 ppm CO

f. Helium mixture with trace amounts of various hydrocarbons:  
~150 ppm each of

|  |   |  |
|--|---|--|
| methane (CH <sub>4</sub> )                       | ethane (C <sub>2</sub> H <sub>6</sub> )   | ethene (C <sub>2</sub> H <sub>4</sub> )  |
| 2methylpropane (C <sub>4</sub> H <sub>10</sub> ) | 1hexene (C <sub>6</sub> H <sub>12</sub> ) | ethyne (C <sub>2</sub> H <sub>2</sub> )  |
| propene (C <sub>3</sub> H <sub>6</sub> )         | propane (C <sub>3</sub> H <sub>8</sub> )  | benzene (C <sub>6</sub> H <sub>6</sub> ) |

g. Helium mixture with large amounts of various noble gases:  
~5% each of xenon and krypton  
~8% argon                      ~25% neon

h. Pure nitrogen(N<sub>2</sub>)

i. Pure hydrogen(H<sub>2</sub>)

---

were unchanged compared to pre-launch values. The synchronizing pulses from the ACP were received correctly.

Future instrument test during the cruise time will be conducted approximately every six months until entry into Titan's atmosphere in 2005. Tuning of the mass spectrometer and vacuum integrity are two of the critical items to be checked. Periodic turn on of the sputter ion pumps is a cautionary step to remove small amounts of residual noble gases, primarily  $^{40}\text{Ar}$ , that are desorbed slowly from surfaces or microscopic cracks where they were trapped during the fabrication of the instrument.

## 5. Expected Results and Measurement Accuracy

The objective of this experiment, as stated above, is the measurement of the chemical composition of the atmosphere of Titan, i.e., the mixing ratio of the major and minor constituents and isotopic ratios when accessible during the Probe descent. The basic accuracy of the measurements and the detection limits of trace gases are determined by the sensitivity of the instrument, the maximum operating pressure of the ion source and the dynamic range of the mass spectrometer. The ion source sensitivity varies with species depending on the ionization cross sections, for example, the sensitivity is about  $1 \times 10^{14}$  counts/s/hPa for molecular nitrogen. Since mixing ratios with respect to nitrogen will be determined, the relative sensitivity to nitrogen has to be obtained by calibration with the relevant gas mixtures.

The background count rate of the secondary electron multiplier ion detectors is less than 0.1 counts per second. An ion source pressure of  $5 \times 10^{-4}$  hPa will be reached at the end of the direct leak 1 and leak 2 measurement phases and during the enrichment cell analysis periods. The exact ion source pressure cannot, of course, be predicted for Ion Source 1 since assumptions had to be made about the descent pressure-time profiles. A maximum ion source pressure of  $1 \times 10^{-3}$  hPa is acceptable.

In the spectral regions where the maximum dynamic range of the instrument can be used, the accuracy will be limited by pulse counting statistics at low mixing ratios. At large mixing ratios where counting statistics become negligible, the measurement accuracy will be  $\pm 2\%$  for peak height ratio measurements of adjacent mass peaks and  $\pm 10\%$  for peak height ratios with wide mass separation. This is because of the error accumulation resulting from calibration uncertainties, small temperature drifts in the supply electronics and change in the gain of the secondary electron multipliers.

In the analysis of gas mixtures, ambiguities in species identification can occur and additional accuracy limitations are expected for species with overlapping mass spectra. Some ambiguities will be resolved by using different energies for the ionizing electron beam. This will only be effective for species with strongly

differing ionization potentials and energy dependent ionization and dissociation cross sections.

The isotopic ratios of hydrogen, carbon and nitrogen will be obtained from the direct methane and nitrogen measurements. The noble gas isotopic ratios will be determined most accurately from the noble gas cell data.

Enrichment factors of 100 in the enrichment cells are expected for ethane and propane and of 500 for higher order hydrocarbons. Krypton and xenon will be enriched approximately 10 times and 100 times, respectively. The actual accuracy can only be established after the data are received and analyzed, because the spectral interference depends on the actual data and background gas uncertainties resulting from the long storage and cruise time.

Mixtures of most low molecular weight hydrocarbons ( $<C_4$ ) and nitriles will be separated by the GC columns and subsequent identification will not be ambiguous if full separation can be achieved. Overlapping eluted peaks will require more careful analysis including simulation on the laboratory calibration system using the Flight Spare instrument.

The basic sensitivity and detector thresholds for the ACP and GC measurements are the same as for the direct measurement. However, since both ACP and GC subsystems are sampling only at several specific times during the Probe descent, a continuous altitude profile of the constituents will not be obtained.

Space flight constraints of low weight, power, and volume put restrictions on the size of the vacuum pumps and thus limit the admissible sample size and the achievable background pressure. The available power for the RF generator for the quadrupole puts limits on the achievable mass resolution. The short descent time also restricts the chance for extensive signal averaging. This is particularly important for traces of reactive gases which may initially be absorbed or decomposed on the surfaces of the sample inlet system before they reach the ionization region. Reactions of hydrogen with loosely bound carbon or oxygen on the vacuum surfaces in the ion source regions cause the formation of methane and water vapor. This effect was significantly suppressed by surface processing, e.g., carbon depletion and formation of stable surface oxides. Methane and water vapor buildup in a hydrogen atmosphere are, however, still limiting the measurement accuracy for these gases in the GC system. IS1 and IS2 will not be affected, of course, by  $H_2$ .

Water vapor measurements are not expected given mixing ratios of  $<10^{-9}$  and the inherent water vapor background in the instrument. Other gases causing chemical noise are carbon monoxide, carbon dioxide and ethane. Carbon monoxide and carbon dioxide form a constant background of several hundred counts per second which does not appear to change significantly when hydrogen enters the ion source. Ethane, on the other hand, does not occur in the background spectrum prior to exposure to hydrogen but it appears in small quantities of 1 ppmv levels when hydrogen enters the ion source. This background level can conceivably change in flight depending on its origin. If ethane is formed in a similar method as methane the background is expected to be the same as during the laboratory tests. Should

ethane slowly accumulate on the vacuum surfaces and be desorbed when hydrogen is introduced, the ethane background could become larger or smaller depending on which process, outgassing or pumping, dominates over the long time period of the cruise phase of the mission. The background level of ethane will ultimately determine the detection threshold of gases with similar fragmentation patterns e.g., ethylene and acetylene.

No background gases or chemical noise are expected above mass 44 at high ion source pressures. Hence constituent measurement accuracy in this region is expected to be determined by the statistical uncertainties associated with the respective sampling times at low concentrations or by the uncertainties caused by temperature drift, etc., to  $\pm 10\%$  as stated above at large concentration levels. Examples of gases which will be detected in this higher, chemically cleaner mass range are krypton, xenon and the higher molecular weight hydrocarbons.

Evaporating cloud droplets of methane or other volatile compounds are expected to be detectable, although quantitative calibration was not possible because facilities to produce droplets in known quantities and size were not available during the calibration period.

### Acknowledgements

The dedication and effort of many people made this complex and difficult experiment possible. The Experimenter Team wishes to acknowledge particularly the contributions of engineers, scientists, technicians and programmers, including R. Abell, R. Arvey, M. Barciniak, R. Bendt, H. Benton, B. Bilodeau, S. Cagiano, E. Campos, C. Carlson, S. Carlson, P. Cursey, S. Dixit, S. Feng, R. Kolecki, C. Lewis, M. McQuaid, A. Melak, V. Navale, M. Paulkovich, E. Patrick, H. Powers, E. Raaen, J. Stuart, F. Tan, J. Thomas, T. Tyler and J. Westberg, at the Goddard Space Flight Center for the design, fabrication, assembly and testing of the gas sampling system, the analyzer system, the digital electronics and the completed instrument. We also acknowledge the engineers, technicians and support staff at the University of Michigan, including K. Arnett, R. Baker, S. Battel, C. Cooper, J. Eder, P. Hansen, M. Huettelman, J. Maurer, R. Miller and S. Raygorodski for the design, fabrication and testing of the analog electronics system; the scientists at the Department of Chemistry at the Ohio State University for the design and development of the low temperature glassy carbon phase (LTGC) column, including Prof. S. Olesik, D. Albaiu and Y. Zhang; D. Coscia and R. Sternberg at the Laboratoire Interuniversitaire des Systemes Atmospheriques of the University of Paris for their contribution to the definition, design, and testing of the gas chromatographic columns.

The manufacturers of major GCMS components include Aker Industries, Oakland, CA (microvalves); Autoflow Products Co., Gardena, CA (pressure regulator); Collimated Holes, Inc., Campbell, CA (glass capillaries); Ergenics, Inc., Ringwood, NJ (hydride metal alloy); Fike Corp., Blue Springs, MO (burst diaphragm);

Galileo Electro Optics, Sturbridge, MA (secondary electron multipliers); Kulite Semiconductor Products, Leonia, NJ, (pressure sensor); Restek Corp., Bellefonte, PA (gas columns); SAES Getters, Colorado Springs, CO (getter material); Supelco, Bellefonte, PA (enrichment cell material); and Teledyne Electronic Technologies, Marina del Rey, CA (hybrids).

At the European Space Research and Technology Centre (ESTEC), we wish to thank the Huygens Probe Project Office for their support and guidance in the program. In particular we are indebted to P. Caseley for his considerable effort as technical coordinator between the Project and the Experimenter Team. We also gratefully acknowledge the very capable management and technical direction provided by H. Hassan, M. Verdant, D. Wyn-Roberts, C. McCarthy and C. Jones at ESTEC and M. Brisson at Aerospatiale. We are indebted to J-P. Lebreton for his excellent leadership as Project Scientist for the Huygens Project.

### References

- Aflalaye A., Sternberg, R., Raulin, F., and Vidal-Madjar, C.: 1995, *J. Chromatogr.* **A708**, 283–291.
- Atreya, S. K.: 1986, *Atmospheres and Ionospheres of the Outer Planets and their Satellites*, Springer-Verlag: New York-Berlin, pp. 166–196.
- Atreya, S. K., Donahue, T. M., and Kuhn, W. R.: 1978, *Science* **212**, 206–211.
- Balsiger H., Altwegg K., and Geiss J.: 1995, *J. of Geophys. Res.-Space Phys.* **100**, 5827–5834.
- Bézard, B., Marten, A., and Paubert, G.: 1993, *Bull. Am. Astron. Soc.* **25**, 1100.
- Bockelee-Morvan, D., Gautier, D., Lis D. C., Young, K., Keene, J., Phillips, T., Owen, T., Crovisier, J., Goldsmith, P. H., Bergin, E. A., Despois, D., and Wooten. A.: 1998, *Icarus* **133**, 147.
- Broadfoot, L. and 15 co-authors.: 1981, *Science* **212**, 206–211.
- de Bergh, C., Lutz, B. L., Owen, T., and Chauville, J.: 1988, *Astrophys. J.* **329**, 951–955.
- Combes, M., Vapillon, L., Gendron, E., Coustenis, A., Lai, O., Wittemberg, R., and Sirdey, R.: 1997, *Icarus* **129**, 482–497.
- Courtin, R., Gautier, D., and McKay, C.: 1995, *Icarus* **114**, 144–162.
- Courtin, R., de Bergh, C., Gautier, D., and Owen, T.: 1998, Paper presented at COSPAR, Nagoya, Japan, July 1998.
- Coustenis, A., Salama, A., Lellouch, E., Encrenaz, T., Bjoraker, G. L., Samuelson, R. E., de Grauw, T., Feichtgruber, H., and Kessler, M. F.: 1998a, *Astron. Astrophysics* **336**, L85–L89.
- Coustenis, A., Encrenaz, T., Salama, A., Lellouch, E., Bjoraker, G., Samuelson, R. E., de Grauw, T., Kestler, M. F., Gautier, D., and Orton, G.: 1998b, *Bull. Am. Astron. Soc.* **30-3**, 1060.
- Coustenis, A. and Bézard, B.: 1995 *Icarus* **115**, 126.
- Coustenis, A., Bézard, B., and Gautier, D.: 1989, *Icarus* **82**, 67–80.
- Dawson, P. H.: 1976, in *Quadrupole Mass Spectrometry and its Applications*, American Vacuum Society Classics, American Institute of Physics Press, New York.
- de Vanssay E., Gazeau, M.-C., Guillemin, J.-C., and Raulin, F.: 1995, *Planet. Space Sci.* **43**, 25–31.
- de Vanssay E., Zubrzycki, S., Sternberg, R., Raulin, F., Sergent, M., and Phan Tan Luu, R.: 1994, *J. Chromatogr.* **688**, 161–170.
- de Vanssay, E., Capilla, P., Coscia, D., Do, L., Sternberg, R., and Raulin, F.: 1993, *J. Chromatogr.* **639**, 255–259.
- Do, L. and Raulin, F.: 1992, *J. Chromatogr.* **591**, 297–301.
- Do, L. and Raulin, F.: 1990, *J. Chromatogr.* **514**, 65–69.
- Do, L. and Raulin, F.: 1989, *J. Chromatogr.* **401**, 45–54.

- Eberhardt, P., Reber, M., Krankowsky, D., Hodges, R. R.: 1995, *Astron. Astrophys.* **302**, 301–316.
- Gautier D. and Owen, T.: 1988, in *Origin and Evolution of Planetary and Satellite Atmospheres*, University of Arizona Press, Tucson, 487–512.
- Gibbard, S. G., Macintosh, B. A., Max, C. E., de Pater, I., Roe, H. G., Marchis, F.: 2001, Paper presented at AAS meeting, December 2001.
- Griffin, M. J. and 30 authors: 1996, *Astron. Astrophys.* **315**, L389–L392.
- Griffith, C. A. and Zahnle, K.: 1995, *J. Geophys. Res.* **100**, 16 907–16 922.
- Guiochon G. and Guillemin, C. L.: 1988, *Quantitative Gas Chromatography*, Elsevier, Amsterdam.
- Gurwell, M. A. and Muhleman, D. O.: 1995, *Icarus* **117**, 375–382.
- Hanel, R. A. and 15 co-authors: 1981, *Science* **212**, 192–200.
- Hidayat, T. A., Marten, A., Bezard, B., Gautier, D., Owen, T., Matthews, H. E., and Paubert, G.: 1997, *Icarus* **126**, 170–182.
- Hidayat, T. A., Marten, A., Bezard, B., Gautier, D., Owen, T., Matthews, H. E., and Paubert, G.: 1998, *Icarus* **133**, 109–133.
- Hunten, D. M., Tomasko, M.G., Flasar, F. M., Samuelson, R. E., Strobel, D. F., and Stevenson, D. J.: 1984, in *SATURN*, Gehrels, T. and Matthews, M. (eds.), University of Arizona Press, Tucson, 671–759.
- Israel, G., Brun, J.-F., Cabane, M., Coscia, D., Niemann, H., Raulin, F., Riedler, W., and Way, S.: 2002 ‘Huygens Probe Aerosol Collector Pyrolyser Experiment’, *Space Sci. Rev.*, **104**, 433–468. this issue
- Kitson, F. G., Larsen, B. S., McEwen, C. N.: 1996, *Gas chromatography and mass spectrometry: a practical guide*, Academic Press, San Diego.
- Kunde, V. G., Aikin, A. C., Hanel, R. A., Jennings, D. E., Maguire, W. C., and Samuelson, R. E.: 1981, *Nature* **292**, 686–688.
- Lara, L. M., Lellouch, E., Lopez-Moreno, J. J., and Rodrigo, R.: 1996, *J. Geophys. Res.* **101**, 23261–23283.
- Lebreton, J.-P. and Matson, D. L.: 2002 ‘The Huygens Probe: Science Payload and Mission Overview’, *Space Science Reviews*, **104**, 59–99.
- Lellouch, E. and Hunten, D. M.: 1997, in *Huygens, Science, Payload, Mission, SP-1177*, A. Wilson (ed.), ESA Publications Division, ESTEC, Noordwijk, The Netherlands, 237–242.
- Lorenz, R. D.: 1993, *ESA Journal* **17**, 275–292.
- Lunine, J.: 1993, *Rev. Geophys. Space Phys.* **31**, 133–149.
- Lunine, J.: 1994, *American Scientist* **82**, 134–143.
- Lunine, J., Atreya, S. K., Pollack, J. B.: 1989, in *Origins and Evolution of Planetary Satellite Atmospheres*, (Atreya, S. K., Pollack, J. B., Matthews, M. S., editors), University of Arizona Press, 605–665.
- Lutz, B. L., de Bergh, C., and Owen, T.: 1983, *Science* **220**, 1374–1375.
- Mahaffy, P. R., Donahue, T. M., Atreya, S. K., Owen, T. C., and Niemann, H. B.: 1998, in *Primordial Nuclei and Their Evolution* (Prantzos, N., Tosi, M., von Steiger, R., editors), Kluwer Academic Publishers, Dordrecht, *in press*. Also, in a Special Issue of, *Space Science Reviews*, *in press*.
- Marten, A., Gautier, D., Tanguy, L., Lecacheux, A., Rosolen, C., and Paubert, G.: 1988, *Icarus* **76**, 558–562.
- Marten, A., Hidayat, T. A., Moreno, R., Paubert, G., Bezard, B., Gautier, D., Matthews, H. E., and Owen, T.: 1997, IAU Circular No. 6702.
- McFadden, W. H.: 1973, *Techniques of Combined Gas Chromatography/Mass Spectrometry*, J. Wiley & Sons, Inc.
- McKay, C. P., Scattergood, T. W., Pollack, J. B., Borucki, W. J., and Van Ghysseghem, H. T.: 1988, *Nature* **6164**, 520–522.
- Meier, R., Owen, T. C., Jewitt, D. C., Matthews, H. E., Matthew, S., Biver, N., Bockelee-Morvan, D., Crovisier, J., and Gautier, D.: 1998, *Science* **279**, 842.

- Morrison, D. M., Owen, T., and Soderblom, L. A.: 1986, in *Satellites*, Burns, J. A. and Matthews, M. S. (eds.) University of Arizona Press, Tucson, 764–801.
- Muhleman, D. O., Grossman, A. W., and Butler, B. J.: 1995, *Ann. Rev. Earth and Planet. Sci.* **23**, 337–374.
- Muhleman, D., Berge, G. L., and Clancey, R. T.: 1984, *Science* **223**, 393.
- Navale, V., Harpold, D., and Vertes, A.: 1998, *Anal. Chem.* **70-4**, 689–697.
- Niemann, H. B., Booth, J. R., Cooley, J. E., Hartle, R. E., Kasprzak, W. T., Spencer, N. W., Way, S. H., Hunten, D. M., and Carignan, G. R.: 1980, *IEEE Transactions on Geoscience and Remote Sensing*, **GE-18-1**, 60–65.
- Niemann, H. B., Harpold, D. N., Atreya, S. K., Carignan, G. R., Hunten, D. M., and Owen, T. C.: 1992, *Space Science Reviews* **60**, 111–142.
- Niemann, H. B., Atreya, S. K., Carignan, G. R., Donahue, T. M., Haberman, J. A., Harpold, D. N., Hartle, R. E., Hunten, D. M., Kasprzak, W. T., Mahaffy, P. R., Owen, T. C., Spencer, N. W., and Way, S. H.: 1996, *Science* **272**, 846–849.
- Noll, K. S., Geballe, T. R., Knacke, R. F., and Pendleton, Y. J.: 1996, *Icarus* **124**, 625–631.
- Orton, G. S.: 1982, in *Proceedings of a Symposium on Titan*, ESA SP-338, 81–88.
- Owen, T.: 1982, *Planet Space Sci.* **30**, 833–838.
- Owen, T. and Bar-Nun, A.: 1995, *Icarus* **116**, 215–226.
- Owen, T. and Gautier, D.: 1989, *Adv. Space Res.* **9**, 73–78.
- Owen, T., Raulin, F., McKay, C., Lunine, J. I., Lebreton, J.-P., and Matson, D. L.: 1997, in *Huygens, Science, Payload, Mission, ESA SP1177*, Wilson, A. (ed.), ESA Publications Division, ESTEC, Noordwijk, The Netherlands, 231–233.
- Owen, T., Meier, R., Matthews, H. E., and Marten, A.: 1998, Paper presented at Symposium in Nantes, France, May 1998: Galileo at Jupiter and Cassini-Huygens at Saturn.
- Raulin F., Frere, C., Paillous, P., de Vanssay, E. Do, L., and Khlifi, M.: 1992a *J. British Interplan. Soc.* **45**, 257–271.
- Raulin F., de Vanssay, E., Do, L., and Paillous, P.: 1992b, *LC-GC* **5**, 22–31.
- Raulin, F., Bruston, P., Paillous, P., and Sternberg, R.: 1995, *Adv. Space Res.* **15**, 321–333.
- Samuelson, R. E., Hanel, R. A., Kunde, V. G., and MaGuire, W. C.: 1981, *Nature* **292**, 688–693.
- Samuelson, R. E. and Maguire, W. C., Hanel, R. A., Kunde, V. G., Jennings, D. E., Yung, Y. L., and Aikin, A.: 1983, *J. Geophys. Res.* **88**, 8709–8715.
- Samuelson, R., Nath, R. A., and Borysow, A.: 1997, *Planetary and Space Science* **45**, 959–980.
- Smith, P. H., Lemmon, M. T., Lorenz, R. D., Sromorsky, J. J., Caldwell, J. J., and Allison, M. D.: 1996, *Icarus* **119**, 336–349.
- Strobel, D. F.: 1982, *Planet. Space Sci.* **30**, 839–848.
- Strobel, D. F., Hall, D. T., Zhu, X., and Summers, M. E.: 1993, *Icarus* **103**, 333–336.
- Toublanc, D., Parisot, J. P., Brillet, J., Gautier, Raulin, F., and McKay, C. P.: 1995, *Icarus* **113**, 2.
- Watson, J. T.: 1997, *Introduction to Mass Spectrometry*, Lippincott-Raven Publishers, 375–398.
- Yung, Y. L., Allen, M., and Pinto, J. P.: 1984, *Astrophys. J. Suppl.* **55**, 465.